Probing new types of P_c states inspired by the interaction between an S-wave charmed baryon and an anticharmed meson in a $\overline{T}$ doublet state

Fu-Lai Wang,[1,2,*] Rui Chen,[1,2,3,4,†] Zhan-Wei Liu [1,2,‡] and Xiang Liu [1,2,§]

[1]*School of Physical Science and Technology, Lanzhou University, Lanzhou 730000, China*
[2]*Research Center for Hadron and CSR Physics, Lanzhou University and Institute of Modern Physics of CAS, Lanzhou 730000, China*
[3]*School of Physics and State Key Laboratory of Nuclear Physics and Technology, Peking University, Beijing 100871, China*
[4]*Center of High Energy Physics, Peking University, Beijing 100871, China*

Inspired by the observations of three P_c states, we systematically investigate interactions between an S-wave charmed baryon $\mathcal{B}_c^{(*)} = \Lambda_c/\Sigma_c/\Sigma_c^*$ and an anticharmed meson $\overline{T} = \bar{D}_1/\bar{D}_2^*$ with the one-pion-exchange potential model and the one-boson-exchange potential model, and search for possible new types of P_c states with the structures of $\mathcal{B}_c^{(*)}\overline{T}$. Both S-D wave mixing and coupled channel effects are considered. Our results suggest that in some $\mathcal{B}_c^{(*)}\overline{T}$ systems there are ideal candidates of new types of P_c states—i.e., the $\Sigma_c\bar{D}_1$ state with $I(J^P) = 1/2(1/2^+)$, the $\Sigma_c\bar{D}_2^*$ state with $I(J^P) = 1/2(3/2^+)$, the $\Sigma_c^*\bar{D}_1$ state with $I(J^P) = 1/2(1/2^+)$, and the $\Sigma_c^*\bar{D}_2^*$ states with $I(J^P) = 1/2(1/2^+, 3/2^+)$—and we suggest that these predicted new types of P_c states can be detected in the process $\Lambda_b^0 \rightarrow \psi(2S)p\pi^-$. Meanwhile, we also extend our study to the interactions between an S-wave charmed baryon and a charmed meson in a T doublet, and we predict a series of double-charm molecular pentaquarks.

I. INTRODUCTION

Exploration of exotic hadronic configurations, which are beyond conventional mesons and baryons in the unquenched quark model, is the academic frontier of hadron physics since these exotic hadronic states have a special position in hadron spectroscopy. Studying exotic hadronic states can provide useful hints to deepen our understanding of the nonperturbative behavior of quantum chromodynamics (QCD). In the past 16 years, experimentalist have observed more and more charmoniumlike XYZ states and P_c states, which have stimulated the development of investigations of exotic hadronic states (see review papers [1–6] for more details).

In March of 2019, the LHCb Collaboration announced new progress on pentaquarks. By revisiting the process $\Lambda_b^0 \rightarrow J/\psi pK$ with the combined data set collected in Run 1 plus Run 2 [7], it was found that three resonance structures, $P_c(4312)$, $P_c(4440)$, and $P_c(4457)$, exist in the $J/\psi p$ invariant mass spectrum. This observation shows that the $P_c(4450)$ structure reported by LHCb in 2015 contains two substructures $P_c(4440)$ and $P_c(4457)$ [8]. This updated result of P_c states provides strong evidence to support the molecular pentaquark [9–48].

When facing such new and exciting results of exploring exotic hadronic states, we propose the question, Where are we going? Let us review the charmoniumlike XYZ from B meson decays. As the first reported charmoniumlike state, $X(3872)$ has inspired extensive discussion of the $D\bar{D}^*$ molecule, which is related to an S-wave charmed meson interacting with an S-wave anticharmed meson. Of course, one must be curious about other hidden-charm charmoniumlike molecular states which are composed of an S-wave charmed meson and a P-wave anticharmed meson. Especially, the observation of $Z(4430)$ directly results in the discussion of whether it can be a $D^*\bar{D}_1$ or $D^*\bar{D}_1'$ molecule [49,50]. Later, our group carried out a systematical calculation of molecular systems composed of an S-wave charmed meson and a P-wave anticharmed meson with $J^P = 0^+, 1^+$ [51], and predicted the possible heavy molecular states from the interaction between a pair of excited charm-strange mesons with $J^P = 0^+$ or 1^+ [52] and a pair of excited charmed mesons $J^P = 1^+$ or 2^+ [53]. The observations of charmoniumlike structures in the $J/\psi\phi$ and $J/\psi\omega$ invariant mass spectra also made us combine these experimental data with former theoretical results to carry out further phenomenological work [54]. To date, more and more higher charmoniumlike XYZ states from B meson weak decays not only make the charmoniumlike XYZ family become abundant, but also inspire interest of researchers in studying the interaction of more highly excited charmed mesons [1].

---

*wangfl2016@lzu.edu.cn

†chen_rui@pku.edu.cn

‡Corresponding author: liuzhanwei@lzu.edu.cn

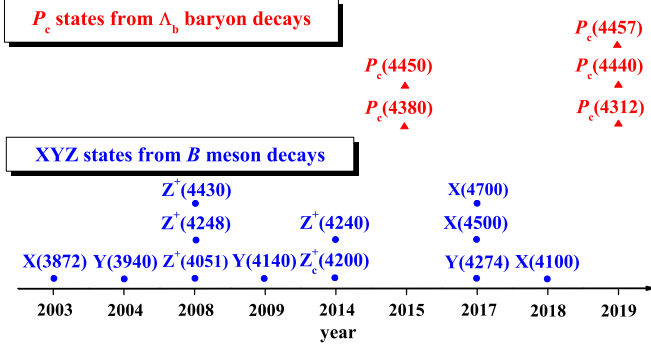§Corresponding author: xiangliu@lzu.edu.cn

FIG. 1. The observed P_c states from Λ_b baryon decays [7,8] and charmoniumlike XYZ states from B meson decays [55–64] with the corresponding first observation year.

When checking the production processes of P_c states from Λ_b baryon decays and XYZ states from B meson decays, there exists a similarity. At present, LHCb has only observed few P_c states, which are closely related to the S-wave charmed meson and S-wave anticharmed baryon (see Fig. 1). According to the experiments behind discovered XYZ states, we have enough reason to believe that more P_c states with larger mass will be reported by LHCb in the near future. Theorists should pay more attention to this interesting issue and give more suggestions for future experimental searches for P_c states. In fact, the present status of the theoretical study of P_c is also similar to that of XYZ states around 2008. Thus, it is a good starting point to investigate how an S-wave charmed baryon interacts with a more highly excited anticharmed meson, by which we can provide valuable information of new types of hidden-charm molecular pentaquarks.

In this work, we will investigate the interactions between an S-wave ground charmed baryon $\mathcal{B}_c^{(*)} = \Lambda_c/\Sigma_c/\Sigma_c^*$ and an anticharmed meson in a $\bar{T}$ doublet $(\bar{D}_1, \bar{D}_2^*)$, where the four P-wave charmed mesons have narrow widths [65]. We also extend our work to study systems with a charmed baryon $\mathcal{B}_c^{(*)}$ and an excited charmed meson D_1/D_2^*. Here, we respectively adopt the one-pion-exchange (OPE) model and the one-boson-exchange (OBE) model, including the exchange contributions from π, σ, η, ρ, and ω in the latter model, which is similar to the study of nuclear force. In addition, the S-D wave mixing effects and coupled channel effects are taken into account in our calculations. We hope that valuable information provided here can be helpful for further experimental searches for the predicted P_c states with larger masses.

This paper is organized as follows. After this Introduction, we present the detailed framework in Sec. II. New types of P_c states with the structures of $\Sigma_c^{(*)}\bar{T}$ and $\Lambda_c\bar{T}$ are given in Secs. III and IV, respectively. In Sec. V, we show the numerical results for doubly charmed molecular pentaquarks. The paper ends with a summary in Sec. VI.

II. FRAMEWORK

To answer whether or not an S-wave ground charmed baryon $\mathcal{B}_c^{(*)} = \Lambda_c/\Sigma_c/\Sigma_c^*$ and an anticharmed meson in $\bar{T}$

doublet $(\bar{D}_1, \bar{D}_2^*)$ can be bound together to form a molecular state, we first investigate the interactions between $\mathcal{B}_c^{(*)}$ and $\bar{D}_1/\bar{D}_2^*$. In this work, we adopt the OPE model and the OBE model, which were developed to study the interactions between hadrons with observed XYZ charmoniumlike states and P_c states [3], to quantitatively describe the strong interactions between $\mathcal{B}_c^{(*)}$ and $\bar{D}_1/\bar{D}_2^*$.

In general, there are three typical steps for extracting the effective potentials which depict the strong interactions between hadrons:

(1) By the effective Lagrangians approach, we can write out the scattering amplitudes $\mathcal{M}(h_1 h_2 \to h_3 h_4)$ of the scattering process $h_1 h_2 \to h_3 h_4$. Later, we list the effective Lagrangians adopted in the present work.

(2) Due to the Breit approximation, the effective potentials in momentum space can be related to the scattering amplitudes, i.e.,

$$\mathcal{V}_E(\boldsymbol{q}) = -\frac{\mathcal{M}(h_1 h_2 \to h_3 h_4)}{\sqrt{\prod_i 2M_i \prod_f 2M_f}}, \qquad (2.1)$$

where $M_{i(f)}$ denotes the mass of the initial (final) state.

(3) By the Fourier transformation, the effective potentials $\mathcal{V}_E(\boldsymbol{q})$ can be transformed into $\mathcal{V}_E(\boldsymbol{r})$ in coordinate space, i.e.,

$$\mathcal{V}_E(\boldsymbol{r}) = \int \frac{d^3\boldsymbol{q}}{(2\pi)^3} e^{i\boldsymbol{q}\cdot\boldsymbol{r}} \mathcal{V}_E(\boldsymbol{q}) \mathcal{F}^2(q^2, m_E^2), \quad (2.2)$$

where m_E and q are the mass and four-momentum of the exchanged particle, respectively. The monopole type form factor $\mathcal{F}(q^2, m_E^2) = (\Lambda^2 - m_E^2)/(\Lambda^2 - q^2)$ [66,67] compensates for the effects from the off-shell exchanged mesons and the more complicated structure of vertices. The cutoff Λ as a phenomenological parameter reflects the intrinsic size of hadrons or the typical hadronic scale. In addition, the introduced form factor also regularizes the effective potentials to cure the ultraviolet singularity.

We can obtain the properties for some possible bound states by solving the Schrödinger equation with the effective potentials.

To write out the relevant scattering amplitudes, one needs the effective Lagrangians to describe the interactions between $\mathcal{B}_c^{(*)}/\bar{D}_1/\bar{D}_2^*$ and the light scalar, pseudoscalar, or vector mesons [68,69], i.e.,

$$\mathcal{L}_{\bar{T}} = g_\sigma'' \langle \overline{T}_a^{(\bar{Q})\mu} \sigma T_{a\mu}^{(\bar{Q})} \rangle + ik \langle \overline{T}_b^{(\bar{Q})\mu} \mathcal{A}_{ba} \gamma_5 T_{a\mu}^{(\bar{Q})} \rangle$$
$$- i\beta'' \langle \overline{T}_{b\lambda}^{(\bar{Q})} v^\mu (\mathcal{V}_\mu - \rho_\mu)_{ba} T_a^{(\bar{Q})\lambda} \rangle$$
$$+ i\lambda'' \langle \overline{T}_{b\lambda}^{(\bar{Q})} \sigma^{\mu\nu} F_{\mu\nu}(\rho)_{ba} T_a^{(\bar{Q})\lambda} \rangle, \qquad (2.3)$$

$$\mathcal{L}_{\mathcal{B}_{\bar{3}}} = l_B \langle \bar{\mathcal{B}}_{\bar{3}} \sigma \mathcal{B}_{\bar{3}} \rangle + i\beta_B \langle \bar{\mathcal{B}}_{\bar{3}} v^\mu (\mathcal{V}_\mu - \rho_\mu) \mathcal{B}_{\bar{3}} \rangle, \qquad (2.4)$$

$$\mathcal{L}_S = l_S \langle \bar{S}_\mu \sigma S^\mu \rangle - \frac{3}{2} g_1 \varepsilon^{\mu\nu\lambda\kappa} v_\kappa \langle \bar{S}_\mu A_\nu S_\lambda \rangle$$
$$+ i\beta_S \langle \bar{S}_\mu v_\alpha (\mathcal{V}^\alpha - \rho^\alpha) S^\mu \rangle + \lambda_S \langle \bar{S}_\mu F^{\mu\nu}(\rho) S_\nu \rangle, \quad (2.5)$$

$$\mathcal{L}_{\mathcal{B}_{\bar{3}} S} = ig_4 \langle \bar{S}^\mu \mathcal{A}_\mu \mathcal{B}_{\bar{3}} \rangle + i\lambda_I \varepsilon^{\mu\nu\lambda\kappa} v_\mu \langle \bar{S}_\nu F_{\lambda\kappa} \mathcal{B}_{\bar{3}} \rangle + \text{H.c.}, \quad (2.6)$$

which can be constructed in heavy quark symmetry and the chiral symmetry [68–73]. Here, $v = (1, \mathbf{0})$ is the four-velocity under the nonrelativistic approximation. The multiplet field T is composed of an axial-vector meson $\bar{D}_1 = (\bar{D}_1^0, D_1^-, D_{s1}^-)^T$ and a tensor meson $\bar{D}_2^* = (\bar{D}_2^{*0}, D_2^{*-}, D_{s2}^{*-})^T$ [69]:

$$T_a^{(\bar{Q})\mu} = \left[\bar{D}_{2a}^{*\mu\nu} \gamma_\nu - \sqrt{\frac{3}{2}} \bar{D}_{1a\nu} \gamma_5 \left(g^{\mu\nu} - \frac{1}{3}(\gamma^\mu - v^\mu)\gamma^\nu \right) \right]$$
$$\times \frac{1 - \slashed{v}}{2}.$$

Its conjugate field satisfies $\overline{T}_a^{(\bar{Q})\mu} = \gamma^0 T_a^{(\bar{Q})\mu\dagger} \gamma^0$. Superfield $\mathcal{S}_\mu$ includes $\mathcal{B}_6$ with $J^P = 1/2^+$ and $\mathcal{B}_6^*$ with $J^P = 3/2^+$ in the 6_F flavor representation, i.e., $\mathcal{S}_\mu = -\sqrt{\frac{1}{3}}(\gamma_\mu + v_\mu)\gamma^5 \mathcal{B}_6 + \mathcal{B}_{6\mu}^*$. Axial current $\mathcal{A}_\mu$ and vector current $\mathcal{V}_\mu$ are defined as $\mathcal{A}_\mu = (\xi^\dagger \partial_\mu \xi - \xi \partial_\mu \xi^\dagger)/2$ and $\mathcal{V}_\mu = (\xi^\dagger \partial_\mu \xi + \xi \partial_\mu \xi^\dagger)/2$, respectively. Here, $\xi = \exp(i\mathbb{P}/f_\pi)$ and $f_\pi = 132$ MeV is for the pion decay constant. In the above formula, vector meson field ρ_μ and its strength tensor $F_{\mu\nu}(\rho)$ are $\rho_\mu = ig_V \mathbb{V}_\mu / \sqrt{2}$ and $F_{\mu\nu}(\rho) = \partial_\mu \rho_\nu - \partial_\nu \rho_\mu + [\rho_\mu, \rho_\nu]$, respectively. Here, matrices $\mathcal{B}_{\bar{3}}$ and $\mathcal{B}_6^{(*)}$ are

$$\mathcal{B}_{\bar{3}} = \begin{pmatrix} 0 & \Lambda_c^+ & \Xi_c^+ \\ -\Lambda_c^+ & 0 & \Xi_c^0 \\ -\Xi_c^+ & -\Xi_c^0 & 0 \end{pmatrix},$$

$$\mathcal{B}_6^{(*)} = \begin{pmatrix} \Sigma_c^{(*)++} & \frac{\Sigma_c^{(*)+}}{\sqrt{2}} & \frac{\Xi_c^{('*)+}}{\sqrt{2}} \\ \frac{\Sigma_c^{(*)+}}{\sqrt{2}} & \Sigma_c^{(*)0} & \frac{\Xi_c^{('*)0}}{\sqrt{2}} \\ \frac{\Xi_c^{('*)+}}{\sqrt{2}} & \frac{\Xi_c^{('*)0}}{\sqrt{2}} & \Omega_c^{(*)0} \end{pmatrix},$$

respectively. Additionally, matrices $\mathbb{P}$ and $\mathbb{V}_\mu$ have the conventional form, which can be found in Ref. [30].

We pick the interaction terms which contain only one light meson by expanding the effective Lagrangians (2.3)–(2.6); such terms are collected in Appendix A.

We need several input parameters to obtain the numerical results. First, the coupling constants existing in Eqs. (2.3)–(2.6) are $l_S = -2l_B = 7.30$, $g_1 = 2\sqrt{2}g_4/3 = 0.94$, $\beta_S g_V = -2\beta_B g_V = -12.00$, $\lambda_S g_V = -2\sqrt{2}\lambda_I g_V = -19.20\,\text{GeV}^{-1}$, and $k = -0.59$ [68], which are widely used to discuss hadronic molecular states [14,30,33]. Here, the coupling constant g_1 can be extracted from the strong decay $\Sigma_c^{(*)} \to \Lambda_c \pi$ [65]. The coupling constant k for $D_1 D_2^* \pi$ vertex is the same as the $DD^*\pi$ coupling constant within the quark model [74], which is determined from the experimental width $\Gamma(D^* \to D\pi)$ [65]. As is well known, information about the coupling constants g_σ'', β'', and λ'' is very scarce at present [69]. In this work, we estimate these coupling constants in the quark model [75], and they can be extracted from the $D^{(*)}$-D^* interactions [30]. Thus, we use $g_\sigma'' = -0.76$, $\beta'' g_V = -5.25$, and $\lambda'' g_V = 3.44\,\text{GeV}^{-1}$ in the following numerical analysis [68,76], and the signs for these coupling constants are fixed by the quark model. In addition, the adopted mass values are $m_\sigma = 600.00$ MeV, $m_\pi = 137.27$ MeV, $m_\eta = 547.85$ MeV, $m_\rho = 775.49$ MeV, $m_\omega = 782.65\,\text{MeV}$, $m_N = 938.27$ MeV, $m_{D_1} = 2422.00$ MeV,

$m_{D_2^*} = 2463.05$ MeV, $m_{\Lambda_c} = 2286.46$ MeV, $m_{\Sigma_c} = 2453.54$ MeV, and $m_{\Sigma_c^*} = 2518.07$ MeV [65]. In our calculation, only the cutoff Λ is a free parameter, and we attempt to find bound state solutions by varying the cutoff parameter in the range of 0.79–4.00 GeV.

In general, the loosely bound states are sensitive to the details of the effective potentials. Because of the uncertainties of the coupling constants g_σ'', β'', and λ'', we should be cautious when studying the existence possibility of the $\mathcal{B}_c^{(*)}\bar{T}$-type hadronic molecular states with the OBE potential model. On the other hand the π exchange interaction, which is clear and widely accepted, contributes to the long-range force in the formation of hadronic molecular states. However, the scalar and vector meson exchange interactions are used to provide the intermediate and short-range contributions, which are not determined very precisely. If the π exchange interaction is dominant and strong enough to generate a loosely bound state, such a loosely bound state can be regarded as a relatively reliable candidate for a hadronic molecular state. Therefore, we study the $\mathcal{B}_c^{(*)}\bar{T}$ molecules within both OPE and OBE models. In our numerical analysis, we first give the numerical results with the OPE potential model. After that, we further take into account other pseudoscalar meson exchange interactions and the scalar and vector meson exchange interactions, and repeat the numerical analysis to check the effects. By comparing the numerical results, we can discuss which bound states are more reliable and less dependent on models.

As is known well, the deuteron is a loosely bound state composed of a proton and a neutron, and may be regarded as an ideal molecular state. Here, we briefly reproduce the binding energy E and root-mean-square radius r_{RMS} for the deuteron via the OPE and OBE models; detailed information on the effective potentials is provided in Ref. [77]. We summarize the numerical results in Table I. A reasonable cutoff in the study of the deuteron is estimated to be around 1.0 GeV, but varies among different scenarios [66,67]. The tensor forces from the S-D wave mixing effects are important for the study of the deuteron. Nevertheless, the S-wave contribution plays the leading role and the D-wave correction is subleading. There are about 95% S-wave and 5% D-wave nucleon-nucleon (NN) in the deuteron, which is consistent with the results from chiral effective field theory [78,79]. In addition, the deuteron is a loosely bound state, and its typical size should be much larger than the size of all the component hadrons. Knowledge of the deuteron helps us to study other molecular states.

TABLE I. Reproducing the binding energy E and root-mean-square radius r_{RMS} for the deuteron with four different scenarios: (A) OPE without S-D mixing effects, (B) OPE with S-D mixing effects, (C) OBE without S-D mixing effects, and (D) OBE with S-D mixing effects.

Models	Λ (GeV)	E (MeV)	r_{RMS} (fm)
OPE(S-D ×)			
OPE(S-D ✓)	1.07	−2.42	3.63
OBE(S-D ×)	1.17	−2.06	3.79
OBE(S-D ✓)	0.87	−2.56	3.58

TABLE II. Flavor wave functions for the discussed $\Sigma_c^{(*)}\bar{T}$ systems. Here, I and I_3 are their isospin and the third components, respectively.

System	$|I, I_3\rangle$	Configurations
$\Sigma_c^{(*)}\bar{T}$	$\left|\frac{3}{2}, \frac{3}{2}\right\rangle$	$|\Sigma_c^{(*)++}T^-\rangle$
	$\left|\frac{3}{2}, \frac{1}{2}\right\rangle$	$\sqrt{\frac{1}{3}}|\Sigma_c^{(*)++}T^-\rangle + \sqrt{\frac{2}{3}}|\Sigma_c^{(*)+}\bar{T}^0\rangle$
	$\left|\frac{3}{2}, -\frac{1}{2}\right\rangle$	$\sqrt{\frac{2}{3}}|\Sigma_c^{(*)+}T^-\rangle + \sqrt{\frac{1}{3}}|\Sigma_c^{(*)0}\bar{T}^0\rangle$
	$\left|\frac{3}{2}, -\frac{3}{2}\right\rangle$	$|\Sigma_c^{(*)0}T^-\rangle$
	$\left|\frac{1}{2}, \frac{1}{2}\right\rangle$	$\sqrt{\frac{2}{3}}|\Sigma_c^{(*)++}T^-\rangle - \sqrt{\frac{1}{3}}|\Sigma_c^{(*)+}\bar{T}^0\rangle$
	$\left|\frac{1}{2}, -\frac{1}{2}\right\rangle$	$\sqrt{\frac{1}{3}}|\Sigma_c^{(*)+}T^-\rangle - \sqrt{\frac{2}{3}}|\Sigma_c^{(*)0}\bar{T}^0\rangle$

III. NEW TYPES OF P_c STATES: $\Sigma_c^{(*)}\bar{D}_1(\bar{D}_2^*)$ SYSTEMS

In this section, we focus on the $\Sigma_c^{(*)}\bar{D}_1(\bar{D}_2^*)$ systems in detail to illustrate how we search for bound states. First, we need to construct the flavor and spin-orbital wave functions for these discussed $\Sigma_c^{(*)}\bar{T}$ pentaquark systems. In Table II, we summarize the flavor wave functions $|I, I_3\rangle$ for the discussed $\Sigma_c^{(*)}\bar{T}$ systems.

For these discussed $\Sigma_c^{(*)}\bar{D}_1(\bar{D}_2^*)$ systems, their spin-orbital wave functions read as

$$|\Sigma_c\bar{D}_1(^{2S+1}L_J)\rangle = \sum_{m,m',m_S m_L} C^{S,m_S}_{\frac{1}{2}m,1m'} C^{J,M}_{Sm_S,Lm_L} \chi_{\frac{1}{2}m} \epsilon^{m'} |Y_{L,m_L}\rangle,$$

$$|\Sigma_c\bar{D}_2^*(^{2S+1}L_J)\rangle = \sum_{m,m'',m_S m_L} C^{S,m_S}_{\frac{1}{2}m,2m''} C^{J,M}_{Sm_S,Lm_L} \chi_{\frac{1}{2}m} \zeta^{m''} |Y_{L,m_L}\rangle,$$

$$|\Sigma_c^*\bar{D}_1(^{2S+1}L_J)\rangle = \sum_{m,m',m_S m_L} C^{S,m_S}_{\frac{3}{2}m,1m'} C^{J,M}_{Sm_S,Lm_L} \Phi_{\frac{3}{2}m} \epsilon^{m'} |Y_{L,m_L}\rangle,$$

$$|\Sigma_c^*\bar{D}_2^*(^{2S+1}L_J)\rangle = \sum_{m,m'',m_S m_L} C^{S,m_S}_{\frac{3}{2}m,2m''} C^{J,M}_{Sm_S,Lm_L} \Phi_{\frac{3}{2}m} \zeta^{m''} |Y_{L,m_L}\rangle,$$

$$(3.1)$$

where $C^{J,M}_{Sm_S,Lm_L}$, $C^{S,m_S}_{\frac{1}{2}m,1m'}$, $C^{S,m_S}_{\frac{1}{2}m,2m''}$, $C^{S,m_S}_{\frac{3}{2}m,1m'}$, and $C^{S,m_S}_{\frac{3}{2}m,2m''}$ are the Clebsch-Gordan coefficients. $|Y_{L,m_L}\rangle$ is the spherical harmonics function. $\chi_{\frac{1}{2}m}$ and $\Phi_{\frac{3}{2}m}$ are defined as the spin wave functions for fermions with $S = 1/2$ and $3/2$, respectively. $\epsilon^{m'}(m' = 0, \pm 1)$ and $\zeta^{m''}(m'' = 0, \pm 1, \pm 2)$ [80] are the polarization vector and tensor, respectively. The explicit expressions for these wave functions are

$$\epsilon^0 = (0, 0, 0, -1),$$

$$\zeta^{m''} = \sum_{m,n} C^{2,m''}_{1m;1n} \epsilon^m \epsilon^n,$$

$$\epsilon^{\pm 1} = \frac{1}{\sqrt{2}}(0, \pm 1, i, 0),$$

$$\Phi_{\frac{3}{2}m} = \sum_{m_1,m_2} C^{\frac{3}{2},m}_{\frac{1}{2}m_1;1m_2} \chi_{\frac{1}{2},m_1} \epsilon^{m_2}. \quad (3.2)$$

With the above preparation, we further write out the spin-orbit wave functions when the S-D wave mixing effects are considered in our calculation, which becomes more com-

plicated. The general expressions corresponding to several typical J^P quantum numbers are

$$|J^P = 1/2^+\rangle: \quad \Sigma_c\bar{D}_1|^2\mathbb{S}_{\frac{1}{2}}/^4\mathbb{D}_{\frac{1}{2}}\rangle,$$

$$\Sigma_c^*\bar{D}_1|^2\mathbb{S}_{\frac{1}{2}}/^4\mathbb{D}_{\frac{1}{2}}/^6\mathbb{D}_{\frac{1}{2}}\rangle,$$

$$\Sigma_c^*\bar{D}_2^*|^2\mathbb{S}_{\frac{1}{2}}/^4\mathbb{D}_{\frac{1}{2}}/^6\mathbb{D}_{\frac{1}{2}}\rangle,$$

$$|J^P = 3/2^+\rangle: \quad \Sigma_c\bar{D}_1|^4\mathbb{S}_{\frac{3}{2}}/^2\mathbb{D}_{\frac{3}{2}}/^4\mathbb{D}_{\frac{3}{2}}\rangle,$$

$$\Sigma_c\bar{D}_2^*|^4\mathbb{S}_{\frac{3}{2}}/^4\mathbb{D}_{\frac{3}{2}}/^6\mathbb{D}_{\frac{3}{2}}\rangle,$$

$$\Sigma_c^*\bar{D}_1|^4\mathbb{S}_{\frac{3}{2}}/^2\mathbb{D}_{\frac{3}{2}}/^4\mathbb{D}_{\frac{3}{2}}/^6\mathbb{D}_{\frac{3}{2}}\rangle,$$

$$\Sigma_c^*\bar{D}_2^*|^4\mathbb{S}_{\frac{3}{2}}/^2\mathbb{D}_{\frac{3}{2}}/^4\mathbb{D}_{\frac{3}{2}}/^6\mathbb{D}_{\frac{3}{2}}/^8\mathbb{D}_{\frac{3}{2}}\rangle,$$

$$|J^P = 5/2^+\rangle: \quad \Sigma_c\bar{D}_2^*|^6\mathbb{S}_{\frac{5}{2}}/^4\mathbb{D}_{\frac{5}{2}}/^6\mathbb{D}_{\frac{5}{2}}\rangle,$$

$$\Sigma_c^*\bar{D}_1|^6\mathbb{S}_{\frac{5}{2}}/^2\mathbb{D}_{\frac{5}{2}}/^4\mathbb{D}_{\frac{5}{2}}/^6\mathbb{D}_{\frac{5}{2}}\rangle,$$

$$\Sigma_c^*\bar{D}_2^*|^6\mathbb{S}_{\frac{5}{2}}/^2\mathbb{D}_{\frac{5}{2}}/^4\mathbb{D}_{\frac{5}{2}}/^6\mathbb{D}_{\frac{5}{2}}/^8\mathbb{D}_{\frac{5}{2}}\rangle,$$

$$|J^P = 7/2^+\rangle: \quad \Sigma_c^*\bar{D}_2^*|^8\mathbb{S}_{\frac{7}{2}}/^4\mathbb{D}_{\frac{7}{2}}/^6\mathbb{D}_{\frac{7}{2}}/^8\mathbb{D}_{\frac{7}{2}}\rangle, \quad (3.3)$$

where the notation $|^{2S+1}L_J\rangle$ is used, in which S, L, and J denote the spin, relative angular momentum, and total angular momentum of the corresponding systems, respectively.

Take the $\Sigma_c\bar{D}_1$ state with $I(J^P) = 1/2(1/2^+)$ as an example to illustrate how we consider the S-D wave mixing effects. The corresponding spatial wave function $|\psi\rangle$, the kinetic term $\mathcal{K}$, and the effective potential $\mathcal{V}$ can be expressed as

$$|\psi\rangle = \left(\Sigma_c\bar{D}_1|^2\mathbb{S}_{\frac{1}{2}}\rangle, \ \Sigma_c\bar{D}_1|^4\mathbb{D}_{\frac{1}{2}}\rangle\right)^T, \quad (3.4)$$

$$\mathcal{K} = \text{diag}\left(-\frac{\nabla^2}{2\mu}, -\frac{\nabla^2}{2\mu} + \frac{3}{\mu r^2}\right), \quad (3.5)$$

$$\mathcal{V} = \begin{pmatrix} \mathcal{V}^{\Sigma_c\bar{D}_1|^2\mathbb{S}_{\frac{1}{2}}\rangle \to \Sigma_c\bar{D}_1|^2\mathbb{S}_{\frac{1}{2}}\rangle} & \mathcal{V}^{\Sigma_c\bar{D}_1|^2\mathbb{S}_{\frac{1}{2}}\rangle \to \Sigma_c\bar{D}_1|^4\mathbb{D}_{\frac{1}{2}}\rangle} \\ \mathcal{V}^{\Sigma_c\bar{D}_1|^4\mathbb{D}_{\frac{1}{2}}\rangle \to \Sigma_c\bar{D}_1|^2\mathbb{S}_{\frac{1}{2}}\rangle} & \mathcal{V}^{\Sigma_c\bar{D}_1|^4\mathbb{D}_{\frac{1}{2}}\rangle \to \Sigma_c\bar{D}_1|^4\mathbb{D}_{\frac{1}{2}}\rangle} \end{pmatrix},$$

$$(3.6)$$

respectively. $\mu = m_{\Sigma_c} m_{D_1}/(m_{\Sigma_c} + m_{D_1})$ is the reduced mass of the $\Sigma_c\bar{D}_1$ system. The superscripts in Eq. (3.6) represent the corresponding scattering processes, which are presented in Appendix B 1. By solving the coupled channel Schrödinger equation, i.e., $(\mathcal{K} + \mathcal{V})|\psi\rangle = E|\psi\rangle$ with E the binding energy, we can obtain the properties of the bound state $\Sigma_c\bar{D}_1$ with $I(J^P) = 1/2(1/2^+)$ as new type of P_c state. Now we can present the numerical results for the $\Sigma_c^{(*)}\bar{D}_1(\bar{D}_2^*)$ systems with the OPE and OBE models, respectively.

A. $\Sigma_c^{(*)}\bar{D}_1(\bar{D}_2^*)$ systems with the OPE model

Generally speaking, the π exchange interaction plays an irreplaceable role in forming loosely bound molecular states. In Table III, we present the binding energy E, root-mean-square (RMS) radius r_{RMS}, and probabilities for different components for the bound states composed of $\Sigma_c\bar{D}_1$ and $\Sigma_c\bar{D}_2^*$ with the OPE model. In order to check the specific roles of the S-D wave mixing effects, we show the numerical results without and with the S-D wave mixing effects.

As shown in Table III, these states can be bound with several MeV binding energy when cutoffs are around 1.1 GeV,

TABLE III. Bound state properties (binding energy E, root-mean-square radius $r_{\rm RMS}$, and probabilities for different components) for the $\Sigma_c \bar{D}_1(\bar{D}_2^*)$ systems with the OPE model. Cutoff Λ, binding energy E, and root-mean-square radius $r_{\rm RMS}$ are in units of GeV, MeV, and fm, respectively. The largest probability of the quantum number configuration for a bound state is indicated by bold typeface. In Tables III–VI and VIII–XI, we use same convention when numerical results are presented: the second column group shows results without considering the S-D wave mixing effects while the last column group shows the relevant results with the S-D wave mixing effects.

$\Sigma_c \bar{D}_1$							
$I(J^P)$	Λ	E	$r_{\rm RMS}$	Λ	E	$r_{\rm RMS}$	$P\left({}^2\mathbb{S}_{\frac{1}{2}}/{}^4\mathbb{D}_{\frac{1}{2}}\right)$
$\frac{1}{2}\left(\frac{1}{2}^+\right)$	1.04	−0.23	4.79	0.99	−0.22	4.92	**99.52**/0.48
	1.15	−3.96	1.55	1.10	−3.65	1.64	**99.05**/0.95
	1.26	−12.69	0.93	1.21	−11.82	1.00	**98.90**/1.10
$I(J^P)$	Λ	E	$r_{\rm RMS}$	Λ	E	$r_{\rm RMS}$	$P\left({}^4\mathbb{S}_{\frac{3}{2}}/{}^2\mathbb{D}_{\frac{3}{2}}/{}^4\mathbb{D}_{\frac{3}{2}}\right)$
$\frac{1}{2}\left(\frac{3}{2}^+\right)$				2.22	−0.27	4.98	**97.06**/0.38/2.56
				2.48	−3.50	1.87	**92.10**/0.95/6.95
				2.74	−12.05	1.13	**88.28**/1.35/10.37
$\frac{3}{2}\left(\frac{3}{2}^+\right)$	3.51	−0.19	4.96	2.22	−0.28	4.68	**98.33**/0.39/1.28
	3.67	−3.88	1.46	2.40	−3.91	1.59	**95.69**/1.00/3.31
	3.83	−12.49	0.84	2.57	−11.97	0.97	**94.01**/1.39/4.60
$\Sigma_c \bar{D}_2^*$							
$I(J^P)$	Λ	E	$r_{\rm RMS}$	Λ	E	$r_{\rm RMS}$	$P\left({}^4\mathbb{S}_{\frac{3}{2}}/{}^4\mathbb{D}_{\frac{3}{2}}/{}^6\mathbb{D}_{\frac{3}{2}}\right)$
$\frac{1}{2}\left(\frac{3}{2}^+\right)$	1.12	−0.19	4.96	1.02	−0.23	4.91	**99.11**/0.12/0.77
	1.24	−4.10	1.51	1.14	−3.80	1.64	**98.16**/0.25/1.59
	1.35	−12.52	0.93	1.26	−12.44	0.99	**97.84**/0.31/1.86
$I(J^P)$	Λ	E	$r_{\rm RMS}$	Λ	E	$r_{\rm RMS}$	$P\left({}^6\mathbb{S}_{\frac{5}{2}}/{}^4\mathbb{D}_{\frac{5}{2}}/{}^6\mathbb{D}_{\frac{5}{2}}\right)$
$\frac{1}{2}\left(\frac{5}{2}^+\right)$				2.13	−0.30	4.88	**96.59**/0.89/2.51
				2.38	−3.72	1.83	**90.75**/2.33/6.92
				2.63	−12.86	1.11	**86.13**/3.41/10.46
$\frac{3}{2}\left(\frac{5}{2}^+\right)$	2.94	−0.27	4.60	2.08	−0.26	4.74	**98.59**/0.57/0.84
	3.09	−3.95	1.45	2.26	−4.05	1.55	**96.36**/1.47/2.16
	3.24	−12.27	0.85	2.43	−12.57	0.94	**95.07**/1.99/2.95

which are reasonable cutoff values. Their RMS radii are all around a few fm, which is consistent with the typical size of a hadronic molecular state. Thus, such loosely bound states can be good candidates of P_c states with larger masses.

In contrast, the π exchange interactions result in repulsive potentials at long range for the $\Sigma_c \bar{D}_1$ states with $I(J^P) = 3/2(1/2^+)$, $1/2(3/2^+)$ and the $\Sigma_c \bar{D}_2^*$ states with $I(J^P) = 3/2(3/2^+)$, $1/2(5/2^+)$, and therefore such states cannot be bound with the OPE model if we do not consider the S-D wave mixing effects. For the $\Sigma_c \bar{D}_1$ state with $I(J^P) = 3/2(3/2^+)$ and the $\Sigma_c \bar{D}_2^*$ state with $I(J^P) = 3/2(5/2^+)$, the OPE potentials are slightly attractive at short range. Compared to the $\Sigma_c \bar{D}_1$ state with $I(J^P) = 3/2(3/2^+)$, the $\Sigma_c \bar{D}_2^*$ state with $I(J^P) = 3/2(5/2^+)$ is more easily bound because of stronger OPE attractions and hadrons with heavier masses, and we can obtain bound solutions for these two states when the cutoffs are taken to be around 3.6 and 3.0 GeV, respectively. In general, a loosely bound state with smaller cutoff corresponds to more attractive force. For the $\Sigma_c \bar{D}_1$ state with $I(J^P) = 1/2(3/2^+)$ and the $\Sigma_c \bar{D}_2^*$ state with $I(J^P) = 1/2(5/2^+)$, these weakly bound state solutions with the cutoff around 2.2 GeV disappear after removing the contributions of the D-wave channels, which implies that the S-D wave mixing effects play an important role in generating these loosely bound states.

Here, recall that the tensor force in the effective potentials plays a critical role in the formation of the loosely bound deuteron.

For the $\Sigma_c \bar{D}_1$ state with $I(J^P) = 3/2(1/2^+)$ and the $\Sigma_c \bar{D}_2^*$ state with $I(J^P) = 3/2(3/2^+)$, there do not exist bound states with the OPE model, even if the S-D wave mixing effects are considered.

Following the procedure discussed above, we present the binding energy, RMS radius, and probabilities for different components for the $\Sigma_c^* \bar{D}_1(\bar{D}_2^*)$ systems with the OPE model in Table IV.

From the numerical results in Table IV, the investigated $\Sigma_c^* \bar{D}_1$ state with $I(J^P) = 1/2(1/2^+)$ and the $\Sigma_c^* \bar{D}_2^*$ states with $I(J^P) = 1/2(1/2^+, 3/2^+)$ can be good candidates of the new types of P_c states since they have small binding energies and suitable RMS radii under reasonable cutoffs, which is because the π exchange interactions give strongly attractive forces around 1.0 fm, and strongly attractive interactions at long range can be used to generate these reasonable loosely bound states. The attractive interactions from the π exchanges contribute at short range for the $\Sigma_c^* \bar{D}_1$ state with $I(J^P) = 3/2(5/2^+)$ and the $\Sigma_c^* \bar{D}_2^*$ state with $I(J^P) = 3/2(7/2^+)$, which makes loosely bound state solutions possible: we find that there exist weakly bound state solutions when the values

TABLE IV. Bound state properties for the $\Sigma_c^*\bar{D}_1(\bar{D}_2^*)$ systems with the OPE model. Conventions are the same as Table III.

System	$I(J^P)$	Λ	E	r_{RMS}	Λ	E	r_{RMS}	$P(^2\mathbb{S}_{\frac{1}{2}}/^4\mathbb{D}_{\frac{1}{2}}/^6\mathbb{D}_{\frac{1}{2}})$
	$\frac{1}{2}(\frac{1}{2}^+)$	0.87	−0.24	4.74	0.82	−0.27	4.08	**99.23**/0.47/0.30
		0.97	−3.92	1.57	0.92	−3.78	1.66	**98.57**/0.89/0.54
		1.07	−12.48	0.96	1.02	−11.93	1.03	**98.38**/ 1.02/0.60
	$\frac{3}{2}(\frac{1}{2}^+)$				3.80	−0.34	4.57	**96.54**/1.62/1.83
					3.90	−1.50	2.55	**93.12**/3.15/3.73
					4.00	−3.75	1.68	**89.55**/4.67/5.78

	$I(J^P)$	Λ	E	r_{RMS}	Λ	E	r_{RMS}	$P(^4\mathbb{S}_{\frac{3}{2}}/^2\mathbb{D}_{\frac{3}{2}}/^4\mathbb{D}_{\frac{3}{2}}/^6\mathbb{D}_{\frac{3}{2}})$
$\Sigma_c^*\bar{D}_1$	$\frac{1}{2}(\frac{3}{2}^+)$	1.84	−0.27	4.59	1.31	−0.24	4.89	**98.24**/0.44/1.19/0.14
		1.98	−4.23	1.43	1.46	−3.78	1.68	**95.84**/1.03/2.82/0.31
		2.11	−12.56	0.87	1.61	−12.53	1.01	**94.53**/1.35/3.72/0.40

	$I(J^P)$	Λ	E	r_{RMS}	Λ	E	r_{RMS}	$P(^6\mathbb{S}_{\frac{5}{2}}/^2\mathbb{D}_{\frac{5}{2}}/^4\mathbb{D}_{\frac{5}{2}}/^6\mathbb{D}_{\frac{5}{2}})$
	$\frac{1}{2}(\frac{5}{2}^+)$				1.98	−0.37	4.65	**95.76**/0.14/0.12/3.97
					2.22	−3.88	1.83	**89.04**/0.26/0.32/10.37
					2.45	−12.50	1.15	**83.55**/0.30/0.48/15.34
	$\frac{3}{2}(\frac{5}{2}^+)$	2.38	−0.24	4.73	1.81	−0.26	4.95	**98.75**/0.18/0.05/1.02
		2.53	−4.11	1.43	1.98	−3.96	1.57	**96.72**/0.47/0.13/2.68
		2.67	−12.33	0.86	2.14	−12.55	0.95	**95.61**/0.63/0.17/3.59

System	$I(J^P)$	Λ	E	r_{RMS}	Λ	E	r_{RMS}	$P(^2\mathbb{S}_{\frac{1}{2}}/^4\mathbb{D}_{\frac{1}{2}}/^6\mathbb{D}_{\frac{1}{2}})$
	$\frac{1}{2}(\frac{1}{2}^+)$	0.82	−0.29	4.55	0.79	−0.75	3.35	**98.82**/0.60/0.58
		0.91	−3.64	1.63	0.88	−4.80	1.52	**98.27**/0.90/0.83
		1.01	−12.29	0.97	0.96	−11.86	1.05	**98.11**/0.99/0.80
	$\frac{3}{2}(\frac{1}{2}^+)$				3.70	−0.56	3.89	**95.89**/1.81/2.31
					3.85	−2.49	2.05	**91.84**/3.52/4.64
					4.00	−6.33	1.36	**87.92**/5.13/6.95

	$I(J^P)$	Λ	E	r_{RMS}	Λ	E	r_{RMS}	$P(^4\mathbb{S}_{\frac{3}{2}}/^2\mathbb{D}_{\frac{3}{2}}/^4\mathbb{D}_{\frac{3}{2}}/^6\mathbb{D}_{\frac{3}{2}}/^8\mathbb{D}_{\frac{3}{2}})$
	$\frac{1}{2}(\frac{3}{2}^+)$	1.11	−0.21	4.86	0.97	−0.28	4.68	**98.68**/0.34/0.62/0.12/0.23
		1.23	−4.16	1.48	1.09	−3.97	1.62	**97.30**/0.71/1.31/0.25/0.43
		1.34	−12.62	0.91	1.21	−12.80	0.99	**96.71**/0.88/1.61/0.30/0.48
	$\frac{3}{2}(\frac{3}{2}^+)$				3.68	−0.26	4.88	**97.15**/0.72/0.96/0.23/0.95
					3.89	−3.11	1.81	**91.51**/2.05/2.69/0.66/3.08
					4.00	−6.29	1.32	**88.66**/2.68/3.50/0.87/4.29

	$I(J^P)$	Λ	E	r_{RMS}	Λ	E	r_{RMS}	$P(^6\mathbb{S}_{\frac{5}{2}}/^2\mathbb{D}_{\frac{5}{2}}/^4\mathbb{D}_{\frac{5}{2}}/^6\mathbb{D}_{\frac{5}{2}}/^8\mathbb{D}_{\frac{5}{2}})$
$\Sigma_c^*\bar{D}_2^*$	$\frac{1}{2}(\frac{5}{2}^+)$				1.57	−0.25	4.93	**97.21**/0.29/0.14/2.29/0.07
					1.75	−3.61	1.79	**92.85**/0.67/0.37/5.96/0.16
					1.93	−12.09	1.07	**89.90**/0.87/0.52/8.49/0.22
	$\frac{3}{2}(\frac{5}{2}^+)$				3.40	−0.27	4.76	**97.81**/0.59/0.15/1.39/0.06
					3.65	−3.77	1.62	**93.73**/1.75/0.45/3.93/0.15
					3.90	−12.49	0.96	**90.50**/2.71/0.69/5.88/0.23

	$I(J^P)$	Λ	E	r_{RMS}	Λ	E	r_{RMS}	$P(^8\mathbb{S}_{\frac{7}{2}}/^4\mathbb{D}_{\frac{7}{2}}/^6\mathbb{D}_{\frac{7}{2}}/^8\mathbb{D}_{\frac{7}{2}})$
	$\frac{1}{2}(\frac{7}{2}^+)$				1.88	−0.29	4.97	**95.75**/ 0.11/ 0.01/ 4.09
					2.12	−3.67	1.89	**88.01**/ 0.22/ 0.14/ 11.62
					2.35	−12.38	1.17	**82.00**/ 0.25/ 0.22/ 17.53
	$\frac{3}{2}(\frac{7}{2}^+)$	2.00	−0.21	4.85	1.63	−0.24	4.81	**98.86**/0.14/0.02/0.98
		2.14	−3.82	1.48	1.79	−4.06	1.54	**97.20**/0.34/0.04/2.42
		2.28	−12.27	0.86	1.94	−12.70	0.93	**96.35**/0.45/0.05/3.15

of the cutoff parameters are taken around 2.4 and 2.0 GeV, respectively. Additionally, the effective potential from the π exchange provides a very weak attractive force for the $\Sigma_c^*\bar{D}_2^*$ state with $I(J^P) = 1/2(5/2^+)$ if we only consider the S-wave component, and we cannot obtain bound state solutions until we increase the cutoff parameter to be around 4.0 GeV.

In contrast to the above situation, the π exchange effective potentials are repulsive for the $\Sigma_c^*\bar{D}_1$ states with

TABLE V. Bound state properties for the $\Sigma_c \bar{D}_1(\bar{D}_2^*)$ systems with the OBE model. Conventions are the same as Table III.

$I(J^P)$	Λ	E	$r_{\rm RMS}$	Λ	E	$r_{\rm RMS}$	$P\left(^2\mathbb{S}_{\frac{1}{2}}/^4\mathbb{D}_{\frac{1}{2}}\right)$
$\frac{1}{2}\left(\frac{1}{2}^+\right)$	0.91	-0.40	4.24	0.88	-0.22	4.98	**99.61**/0.39
	1.01	-5.07	1.49	0.98	-4.65	1.57	**99.20**/0.80
	1.10	-12.30	1.05	1.07	-12.28	1.07	**99.04**/0.96
$\frac{3}{2}\left(\frac{1}{2}^+\right)$	2.106	-0.48	3.27	1.96	-1.64	2.06	**89.81**/10.19
	2.112	-5.63	0.79	1.97	-5.30	1.14	**86.95**/13.05
	2.118	-12.02	0.53	1.98	-10.20	0.84	**85.98**/ 14.02

$I(J^P)$	Λ	E	$r_{\rm RMS}$	Λ	E	$r_{\rm RMS}$	$P\left(^4\mathbb{S}_{\frac{3}{2}}/^2\mathbb{D}_{\frac{3}{2}}/^4\mathbb{D}_{\frac{3}{2}}\right)$
$\frac{1}{2}\left(\frac{3}{2}^+\right)$	1.59	-0.26	4.99	1.24	-0.35	4.71	**97.88**/0.34/1.78
	1.78	-4.11	1.68	1.35	-3.93	1.83	**94.91**/0.81/4.29
	1.97	-12.71	1.04	1.46	-12.24	1.16	**92.92**/1.11/5.97
$\frac{3}{2}\left(\frac{3}{2}^+\right)$				2.02	-0.40	4.28	**94.71**/1.32/3.97
				2.11	-4.55	1.58	**86.34**/3.50/10.16
				2.19	-12.28	1.07	**81.06**/4.98/13.96

$\Sigma_c \bar{D}_2^*$

$I(J^P)$	Λ	E	$r_{\rm RMS}$	Λ	E	$r_{\rm RMS}$	$P\left(^4\mathbb{S}_{\frac{3}{2}}/^4\mathbb{D}_{\frac{3}{2}}/^6\mathbb{D}_{\frac{3}{2}}\right)$
$\frac{1}{2}\left(\frac{3}{2}^+\right)$	0.94	-0.38	4.32	0.90	-0.37	4.38	**99.21**/0.11/0.68
	1.04	-5.39	1.46	0.99	-4.39	1.62	**98.53**/0.21/1.26
	1.14	-12.36	1.05	1.08	-11.98	1.09	**98.21**/0.26/1.53
$\frac{3}{2}\left(\frac{3}{2}^+\right)$	2.202	-0.66	2.65	1.93	-1.01	2.76	**90.84**/1.95/7.21
	2.208	-5.92	0.75	1.95	-5.75	1.19	**85.30**/3.19/11.51
	2.214	-12.27	0.52	1.96	-9.21	0.96	**84.13**/3.48/12.40

$I(J^P)$	Λ	E	$r_{\rm RMS}$	Λ	E	$r_{\rm RMS}$	$P\left(^6\mathbb{S}_{\frac{5}{2}}/^4\mathbb{D}_{\frac{5}{2}}/^6\mathbb{D}_{\frac{5}{2}}\right)$
$\frac{1}{2}\left(\frac{5}{2}^+\right)$	1.65	-0.30	4.78	1.24	-0.29	4.93	**97.72**/0.69/1.58
	1.84	-4.21	1.66	1.35	-3.80	1.86	**94.09**/1.78/4.13
	2.02	-12.61	1.03	1.46	-12.32	1.16	**91.58**/2.52/5.89
$\frac{3}{2}\left(\frac{5}{2}^+\right)$				2.08	-0.22	5.02	**96.24**/1.64/2.12
				2.18	-3.89	1.69	**88.61**/5.11/6.28
				2.28	-12.54	1.07	**83.14**/7.79/9.07

$I(J^P) = 3/2(1/2^+, 3/2^+), 1/2(5/2^+)$ and the $\Sigma_c^* \bar{D}_2^*$ states with $I(J^P) = 3/2(1/2^+, 3/2^+, 5/2^+), 1/2(7/2^+)$, and there do not exist bound state solutions with the OPE model if the contributions of the D-wave channels are not considered. The tensor forces from the S-D wave mixing effects are essential in the formation of these loosely bound states. There are no bound solutions for the $\Sigma_c^* \bar{D}_1$ state with $I(J^P) = 3/2(3/2^+)$ with the OPE model, even if we consider the S-D wave mixing effects.

B. $\Sigma_c^{(*)} \bar{D}_1(\bar{D}_2^*)$ systems with the OBE model

Usually, the pion exchange interaction plays a dominant role in forming the loosely bound states at long range due to the molecular state being a loosely bound state; the interactions from other light meson exchanges, especially the vector exchange interaction, may play an important role to modify the bound state properties to a large extent at intermediate and short ranges. In fact, the η exchange interaction usually plays a minor role in generating the loosely bound states [81], and the contribution from the σ exchange always gives an attractive force [82].

The OBE model is a little more complex, and we carry out an analysis similar to that for OPE. For the $\Sigma_c \bar{D}_1$ and $\Sigma_c \bar{D}_2^*$ systems, the π, σ, η, ρ, and ω exchanges contribute to the total effective potentials. In Table V, we present the corresponding bound properties for the $\Sigma_c \bar{D}_1$ and $\Sigma_c \bar{D}_2^*$ systems within the OBE model.

As shown in Table V, we can obtain more loosely bound states with reasonable cutoffs after considering the scalar and vector meson exchange effective potentials. For the $\Sigma_c \bar{D}_1$ state with $I(J^P) = 1/2(1/2^+)$ and the $\Sigma_c \bar{D}_2^*$ state with $I(J^P) = 1/2(3/2^+)$, we find loosely bound state solutions within reasonable cutoffs for both the OPE model and the OBE model, and the energies and radii are similar, which means that the total effective potentials mainly come from the π exchanges, and the scalar and vector meson exchange effective potentials play a minor role in the formation of these bound states when cutoff parameters Λ are around 0.95 GeV. Therefore, we conclude that the $\Sigma_c \bar{D}_1$ state with $I(J^P) = 1/2(1/2^+)$ and the $\Sigma_c \bar{D}_2^*$ state with $I(J^P) = 1/2(3/2^+)$ are favored to be the better candidates of the new types of P_c states. By comparing the numerical results of the OPE model, the cutoffs are relatively more reasonable for the loosely

bound states in the $\Sigma_c \bar{D}_1$ system with $I(J^P) = 1/2(3/2^+)$ and the $\Sigma_c \bar{D}_2^*$ system with $I(J^P) = 1/2(5/2^+)$ within OBE model. Here, the ρ and ω exchange attractive forces play a significant role in the formation of these loosely bound states with cutoffs of about 1.65 GeV.

The binding energies of the $\Sigma_c \bar{D}_1$ state with $I(J^P) = 3/2(1/2^+)$ and the $\Sigma_c \bar{D}_2^*$ state with $I(J^P) = 3/2(3/2^+)$ are very sensitive to the cutoffs, which differs from other states greatly. The main reason is that the ρ and ω exchange interactions give strongly attractive forces at relatively short range when the cutoff parameter Λ is around 2.2 GeV, and there are almost no attractive forces at intermediate and long ranges. Especially, the effective potentials related to the $\mathbf{q}^2/(q^2 + m^2)$ term in momentum space have a great influence on these bound states, and the short-range dynamics make the numerical results more sensitive to the values of the cutoffs.

In many $\Sigma_c \bar{D}_1(\bar{D}_2^*)$ systems, the binding energy in the OBE model is larger than that in the OPE model with the same cutoff parameters since the intermediate and short-range interactions often play an essential role in the formation of the loosely bound states. Comparing the results with and without the S-D wave mixing effects, it is obvious that the S-D wave mixing effects are important in the formation of several molecular states, especially for the $\Sigma_c \bar{D}_1$ state with $I(J^P) = 3/2(3/2^+)$ and the $\Sigma_c \bar{D}_2^*$ state with $I(J^P) = 3/2(5/2^+)$.

Similarly to the $\Sigma_c \bar{D}_1(\bar{D}_2^*)$ systems, we present the bound properties for the $\Sigma_c^* \bar{D}_1(\bar{D}_2^*)$ systems with the OBE model in Table VI. From Tables VI and IV, it is obvious that the bound state properties will change accordingly after we consider the contributions from the scalar and vector meson exchange effective potentials.

We can obtain loosely bound states in the $\Sigma_c^* \bar{D}_1$ system with $I(J^P) = 1/2(1/2^+)$ and the $\Sigma_c^* \bar{D}_2^*$ system with $I(J^P) = 1/2(1/2^+, 3/2^+)$ with the cutoffs around 1.00 GeV by using both the OPE model and the OBE model. Different from the OPE case, the ρ and ω exchange attractive forces play an important role in the formation of the $\Sigma_c^* \bar{D}_1$ states with $I(J^P) = 1/2(3/2^+, 5/2^+)$ and the $\Sigma_c^* \bar{D}_2^*$ state with $I(J^P) = 1/2(5/2^+, 7/2^+)$, and they are loosely bound molecular states with the OBE model, especially when we consider the contributions of the D-wave channels. The situation of the $\Sigma_c^* \bar{D}_1$ states with $I(J^P) = 3/2(1/2^+, 3/2^+)$ and the $\Sigma_c^* \bar{D}_2^*$ states with $I(J^P) = 3/2(1/2^+, 3/2^+)$ is similar to that of the $\Sigma_c \bar{D}_1$ state with $I(J^P) = 3/2(1/2^+)$ and the $\Sigma_c \bar{D}_2^*$ state with $I(J^P) = 3/2(3/2^+)$ qualitatively, and their properties significantly depend sensitively on the cutoff parameter, and thus our results indicate that these bound states cannot be good candidates of hadronic molecular states.

C. Discussion and rating for bound states

The D-wave components with small contributions does not obviously change some bound state properties [53]. However, for the $\Sigma_c^{(*)} \bar{D}_1(\bar{D}_2^*)$ states with $I = 3/2$ and others, their bound state properties may change considerably after considering the S-D wave mixing effects, which is mainly determined by the nondiagonal matrix elements of the effective potentials [83].

The states with $I = 1/2$ are easier to bind as a hadronic molecular candidate than those with $I = 3/2$ for the low

spin $\Sigma_c^{(*)} \bar{T}$-type systems. This is not surprising since the π exchange effective potentials are weakly repulsive with $I = 3/2$ and strongly attractive with $I = 1/2$ for the low spin hidden-charm pentaquark states.

Empirically, the vector exchange interaction may be important for the formation of hadronic molecular states if the cutoff parameter is greater than 1.5 GeV; this is due to the introduction of the form factor $\mathcal{F}(q^2, m_E^2) = (\Lambda^2 - m_E^2)/(\Lambda^2 - q^2)$ into the effective potential in the present work. Of course, when the cutoff parameter is relatively small, it is obvious that the π exchange interaction plays an irreplaceable role in generating these loosely bound molecular states.

As shown in Tables III–VI, we can predict a series of possible new types of P_c states with the form $\Sigma_c^{(*)} \bar{T}$. We have considered four different scenarios: (A) OPE without S-D mixing effects, (B) OPE with S-D mixing effects, (C) OBE without S-D mixing effects, and (D) OBE with S-D mixing effects. We notice that some bound states exist in some scenarios but disappear in other scenarios. Shall we treat them equally?

Many hadron molecular states have been predicted by different theoretical groups, and we try to categorize them in some reasonable way and give a rough indication which states deserve experimental resources.

If a bound state can be formed both with and without D-wave contributions, it means that the convergence of partial-wave expansion is good and thus the results are more reliable in our scheme. For similar reasons, the states bound within both OPE and OBE models have smaller theoretical uncertainties.

Therefore, we provide a preliminary rating scheme. If a bound state can exist in n scenarios with reasonable cutoff around 1.0 GeV, we rate it as an n-star state. For example, $\Sigma_c^* \bar{D}_1$ with $I(J^P) = 1/2(3/2^+)$ can be bound in scenarios (B), (C), and (D), and thus we assign it three stars. In this rating system, $P_c(4440)$ is a four-star state. In Table VII we present our rating for new types of P_c states in $\Sigma_c^{(*)} \bar{D}_1(\bar{D}_2^*)$ systems.

In this rating scheme, the deuteron has only three stars but is still in the top two among five ranks. There are many zero-star states which cannot be bond in any scenario and are not listed in Table VII. However, in an ideal rating scheme the deuteron should most probably be in the top rank. The rating scheme in this paper definitely needs efforts from particle physicists to be improved in future.

To investigate the uncertainties of cutoff for these four-star states within the OPE model and OBE model, in Fig. 2 we present the Λ dependence of the binding energy and root-mean-square radius for two typical states, $\Sigma_c \bar{D}_1$ with $I(J^P) = 1/2(1/2^+)$ and $\Sigma_c \bar{D}_2^*$ with $I(J^P) = 1/2(3/2^+)$. We can see clearly that the binding properties of these four-star states are not significantly dependent on the cutoff Λ.

In comparison to those large spin states, we find that the low spin states may be bound more tightly for the $\Sigma_c^{(*)} \bar{D}_1(\bar{D}_2^*)$ states with $I = 1/2$, which have results similar to the $\Sigma_c^{(*)} \bar{D}^{(*)}$ states with $I = 1/2$ [30]. The observations of three resonance structures, $P_c(4312)$, $P_c(4440)$, and $P_c(4457)$, are from the Λ_b baryon decays [7], and thus one can search for these predicted new types of P_c states through the Λ_b baryon weak

TABLE VI. Bound state properties for the $\Sigma_c^* \bar{D}_1 (\bar{D}_2^*)$ systems with the OBE model. Conventions are the same as Table III.

System	$I(J^P)$	Λ	E	r_{RMS}	Λ	E	r_{RMS}	$P\left(^2\mathbb{S}_{\frac12}/^4\mathbb{D}_{\frac12}/^6\mathbb{D}_{\frac12}\right)$
	$\frac12\left(\frac12^+\right)$	0.82	-0.31	4.50	0.79	-0.35	4.40	**99.26**/0.45/0.29
		0.91	-4.68	1.52	0.88	-4.72	1.56	**98.71**/0.80/0.49
		1.00	-12.98	1.02	0.96	-12.49	1.06	**98.51**/0.93/0.56
	$\frac32\left(\frac12^+\right)$	1.917	-0.29	4.42	1.71	-0.25	4.73	**93.76**/2.85/3.39
		1.923	-5.51	0.82	1.73	-4.11	1.43	**84.65**/6.96/8.39
		1.929	-12.21	0.54	1.75	-11.55	0.90	**81.92**/8.25/9.84

	$I(J^P)$	Λ	E	r_{RMS}	Λ	E	r_{RMS}	$P\left(^4\mathbb{S}_{\frac32}/^2\mathbb{D}_{\frac32}/^4\mathbb{D}_{\frac32}/^6\mathbb{D}_{\frac32}\right)$
	$\frac12\left(\frac32^+\right)$	1.09	-0.36	4.44	1.00	-0.41	4.32	**98.63**/0.36/0.91/0.11
		1.22	-5.06	1.51	1.10	-4.69	1.62	**97.15**/0.75/1.89/0.21
$\Sigma_c^* \bar{D}_1$		1.34	-12.54	1.05	1.19	-12.08	1.12	**96.37**/0.95/ 2.42/0.26
	$\frac32\left(\frac32^+\right)$	2.979	-0.36	3.49	2.02	-0.54	3.71	**92.95**/2.58/3.89/0.58
		2.985	-5.80	0.67	2.06	-5.86	1.27	**84.19**/5.91/8.62/1.28
		2.991	-12.26	0.45	2.09	-13.10	0.90	**80.98**/7.21/10.31/1.50

	$I(J^P)$	Λ	E	r_{RMS}	Λ	E	r_{RMS}	$P\left(^6\mathbb{S}_{\frac52}/^2\mathbb{D}_{\frac52}/^4\mathbb{D}_{\frac52}/^6\mathbb{D}_{\frac52}\right)$
	$\frac12\left(\frac52^+\right)$	1.74	-0.29	4.86	1.24	-0.38	4.61	**97.00**/0.15/0.10/2.75
		1.92	-3.85	1.72	1.35	-4.18	1.80	**92.61**/0.33/0.23/6.82
		2.10	-12.63	1.02	1.45	-12.36	1.18	**89.80**/0.42/0.33/9.45
	$\frac32\left(\frac52^+\right)$				1.99	-0.38	4.36	**95.62**/0.79/0.19/3.40
					2.10	-4.40	1.63	**88.59**/2.18/0.50/8.72
					2.20	-12.30	1.10	**83.91**/3.26/0.73/12.10

System	$I(J^P)$	Λ	E	r_{RMS}	Λ	E	r_{RMS}	$P\left(^2\mathbb{S}_{\frac12}/^4\mathbb{D}_{\frac12}/^6\mathbb{D}_{\frac12}\right)$
$\Sigma_c^* \bar{D}_2^*$	$\frac12\left(\frac12^+\right)$	0.79	-0.40	4.16	0.79	-1.57	2.47	**98.74**/0.64/0.62
		0.88	-5.12	1.46	0.86	-6.19	1.40	**98.42**/0.82/0.76
		0.96	-12.96	1.01	0.92	-12.60	1.06	**98.26**/0.91/0.83
	$\frac32\left(\frac12^+\right)$	1.860	-0.67	2.69	1.65	-0.33	4.40	**93.70**/2.71/3.59
		1.866	-6.33	0.77	1.67	-4.24	1.42	**85.61**/6.17/8.22
		1.871	-12.09	0.55	1.69	-11.81	0.90	**83.01**/7.32/8.67

	$I(J^P)$	Λ	E	r_{RMS}	Λ	E	r_{RMS}	$P\left(^4\mathbb{S}_{\frac32}/^2\mathbb{D}_{\frac32}/^4\mathbb{D}_{\frac32}/^6\mathbb{D}_{\frac32}/^8\mathbb{D}_{\frac32}\right)$
	$\frac12\left(\frac32^+\right)$	0.93	-0.28	4.64	0.87	-0.25	4.85	**98.96**/0.27/0.49/0.10/0.18
		1.03	-4.52	1.55	0.96	-4.12	1.66	**97.84**/0.58/1.03/0.20/0.35
		1.13	-12.14	1.04	1.05	-12.04	1.09	**97.30**/0.73/1.31/0.25/0.41
	$\frac32\left(\frac32^+\right)$	2.194	-0.61	2.74	1.78	-0.24	4.77	**94.09**/1.40/7.84/0.46/2.21
		2.200	-5.86	0.74	1.81	-4.38	1.42	**84.22**/3.74/4.83/1.21/6.01
		2.206	-12.22	0.50	1.84	-12.87	0.88	**80.40**/4.70/6.00/1.49/7.40

	$I(J^P)$	Λ	E	r_{RMS}	Λ	E	r_{RMS}	$P\left(^6\mathbb{S}_{\frac52}/^2\mathbb{D}_{\frac52}/^4\mathbb{D}_{\frac52}/^6\mathbb{D}_{\frac52}/^8\mathbb{D}_{\frac52}\right)$
	$\frac12\left(\frac52^+\right)$	1.23	-0.24	4.98	1.07	-0.37	4.52	**98.08**/0.25/0.11/1.52/0.04
		1.38	-4.37	1.61	1.17	-4.26	1.71	**95.68**/0.53/0.24/3.46/0.09
		1.53	-12.15	1.06	1.27	-12.41	1.12	**94.19**/0.68/0.32/4.68/0.13
	$\frac32\left(\frac52^+\right)$				2.07	-0.27	4.73	**95.08**/1.46/0.36/2.97/0.12
					2.13	-4.56	1.47	**85.84**/4.41/1.07/8.35/0.34
					2.18	-12.17	0.98	**81.25**/6.03/1.43/0.86/0.43

	$I(J^P)$	Λ	E	r_{RMS}	Λ	E	r_{RMS}	$P\left(^8\mathbb{S}_{\frac72}/^4\mathbb{D}_{\frac72}/^6\mathbb{D}_{\frac72}/^8\mathbb{D}_{\frac72}\right)$
	$\frac12\left(\frac72^+\right)$	1.83	-0.29	4.85	1.24	-0.36	4.71	**96.65**/0.13/0.05/3.17
		2.00	-3.74	1.72	1.35	-4.10	1.82	**91.44**/0.29/0.13/8.15
		2.16	-12.16	1.11	1.45	-12.47	1.17	**88.03**/0.36/0.18/11.43
	$\frac32\left(\frac72^+\right)$				1.98	-0.32	4.50	**96.24**/0.63/0.04/3.09
					2.10	-3.98	1.70	**89.94**/1.82/0.12/8.12
					2.22	-12.19	1.10	**85.31**/2.86/0.17/11.66

TABLE VII. Rating for new types of P_c states in $\Sigma_c^{(*)}\bar{D}_1(\bar{D}_2^*)$ systems with (I, J).

Rating	$\Sigma_c\bar{D}_1$	$\Sigma_c\bar{D}_2^*$	$\Sigma_c^*\bar{D}_1$	$\Sigma_c^*\bar{D}_2^*$
★★★★	$(\frac{1}{2}, \frac{1}{2})$	$(\frac{1}{2}, \frac{3}{2})$	$(\frac{1}{2}, \frac{1}{2})$	$(\frac{1}{2}, \frac{1}{2}/\frac{3}{2})$
★★★			$(\frac{1}{2}, \frac{3}{2})$	$(\frac{1}{2}, \frac{5}{2}), (\frac{3}{2}, \frac{7}{2})$
★★	$(\frac{1}{2}, \frac{3}{2})$			
★		$(\frac{1}{2}, \frac{5}{2})$	$(\frac{1}{2}, \frac{5}{2})$	$(\frac{1}{2}, \frac{7}{2})$

decays reported by the LHCb Collaboration. By simple partial wave analysis, we suggest first searching for these low spin $\Sigma_c^{(*)}\bar{D}_1(\bar{D}_2^*)$ states with $I = 1/2$ in the future. For these new types of P_c states with the structures of $\Sigma_c\bar{D}_1$, $\Sigma_c\bar{D}_2^*$, $\Sigma_c^*\bar{D}_1$, and $\Sigma_c^*\bar{D}_2^*$, the masses were predicted to be around 4.87, 4.91, 4.93, and 4.97 GeV, respectively.

IV. NEW TYPE OF P_c STATES: $\Lambda_c\bar{D}_1(\bar{D}_2^*)$ SYSTEMS

In this section, we study the $\Lambda_c\bar{D}_1(\bar{D}_2^*)$ systems only within the OBE model since the pion exchange interaction is forbidden because of spin-parity conservation. In addition, there are no tensor force in the effective potentials for the $\Lambda_c\bar{D}_1(\bar{D}_2^*)$ systems (see Appendix B 2 for more details), and therefore we do not consider the S-D wave mixing effects in this investigation.

The interactions of the $\Lambda_c\bar{D}_1(\bar{D}_2^*)$ systems are quite simple, because spin-parity conservation forbids the vertexes $\Lambda_c\Lambda_c\pi/\eta/\rho$. Thus there are only ω and σ exchange interactions. Moreover, the ω exchange potentials are repulsive while the σ exchange potentials are attractive, and thus the total potentials are very shallow. In fact, we cannot find the bound states for the $\Lambda_c\bar{D}_1$ systems with $I(J^P) = 1/2(1/2^+, 3/2^+)$ and the $\Lambda_c\bar{D}_2^*$ systems with $I(J^P) = 1/2(3/2^+, 5/2^+)$ when cutoffs Λ are tuned from 0.79 to 4.00 GeV. This is similar to the results of the $\Lambda_c\bar{D}^{(*)}$ systems; that is, Λ_c does not combine
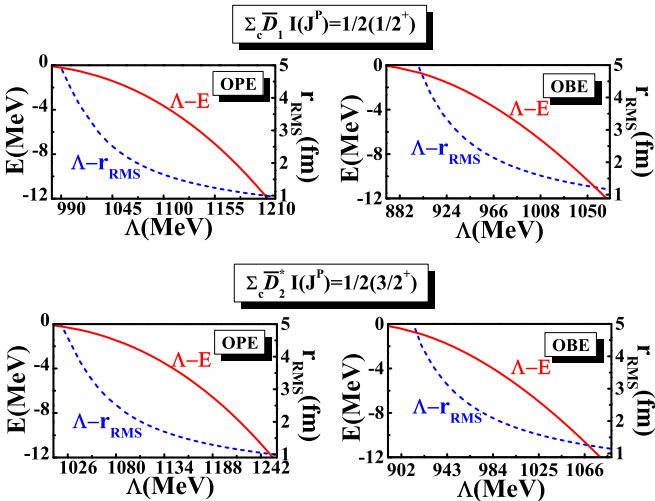
with $\bar{D}^{(*)}$ to form hidden-charm molecular pentaquarks for the single-channel calculations [26].

Since the pion exchange interactions are allowed for the processes $\Lambda_c\bar{T} \to \Sigma_c^{(*)}\bar{T}$, we expect that the coupled channel effects play an important role to generate the loosely bound hidden-charm molecular states for the $\Lambda_c\bar{T}$ systems. Thus, we further briefly discuss the $\mathcal{B}_c^{(*)}\bar{T}$ coupled systems. In the coupled channel analysis, the binding energy is provided relative to the lowest-lying threshold [84].

Take the $\mathcal{B}_c^{(*)}\bar{T}$ coupled systems with $I(J^P) = 1/2(1/2^+)$ as an example. The corresponding spatial wave function $|\psi\rangle$, the kinetic term $\mathcal{K}$, and the effective potential $\mathcal{V}$ can be written as

$$|\psi\rangle = (|\Lambda_c\bar{D}_1\rangle, |\Sigma_c\bar{D}_1\rangle, |\Sigma_c^*\bar{D}_1\rangle, |\Sigma_c^*\bar{D}_2^*\rangle)^T, \quad (4.1)$$

$$\mathcal{K} = \mathrm{diag}\left(-\frac{\nabla^2}{2\mu_1}, -\frac{\nabla^2}{2\mu_2} + d_1, -\frac{\nabla^2}{2\mu_3} + d_2, -\frac{\nabla^2}{2\mu_4} + d_3\right), \quad (4.2)$$

$$\mathcal{V} = \begin{pmatrix} \mathcal{V}^{\Lambda_c\bar{D}_1 \to \Lambda_c\bar{D}_1} & \mathcal{V}^{\Lambda_c\bar{D}_1 \to \Sigma_c\bar{D}_1} & \mathcal{V}^{\Lambda_c\bar{D}_1 \to \Sigma_c^*\bar{D}_1} & \mathcal{V}^{\Lambda_c\bar{D}_1 \to \Sigma_c^*\bar{D}_2^*} \\ \mathcal{V}^{\Sigma_c\bar{D}_1 \to \Lambda_c\bar{D}_1} & \mathcal{V}^{\Sigma_c\bar{D}_1 \to \Sigma_c\bar{D}_1} & \mathcal{V}^{\Sigma_c\bar{D}_1 \to \Sigma_c^*\bar{D}_1} & \mathcal{V}^{\Sigma_c\bar{D}_1 \to \Sigma_c^*\bar{D}_2^*} \\ \mathcal{V}^{\Sigma_c^*\bar{D}_1 \to \Lambda_c\bar{D}_1} & \mathcal{V}^{\Sigma_c^*\bar{D}_1 \to \Sigma_c\bar{D}_1} & \mathcal{V}^{\Sigma_c^*\bar{D}_1 \to \Sigma_c^*\bar{D}_1} & \mathcal{V}^{\Sigma_c^*\bar{D}_1 \to \Sigma_c^*\bar{D}_2^*} \\ \mathcal{V}^{\Sigma_c^*\bar{D}_2^* \to \Lambda_c\bar{D}_1} & \mathcal{V}^{\Sigma_c^*\bar{D}_2^* \to \Sigma_c\bar{D}_1} & \mathcal{V}^{\Sigma_c^*\bar{D}_2^* \to \Sigma_c^*\bar{D}_1} & \mathcal{V}^{\Sigma_c^*\bar{D}_2^* \to \Sigma_c^*\bar{D}_2^*} \end{pmatrix}, \quad (4.3)$$
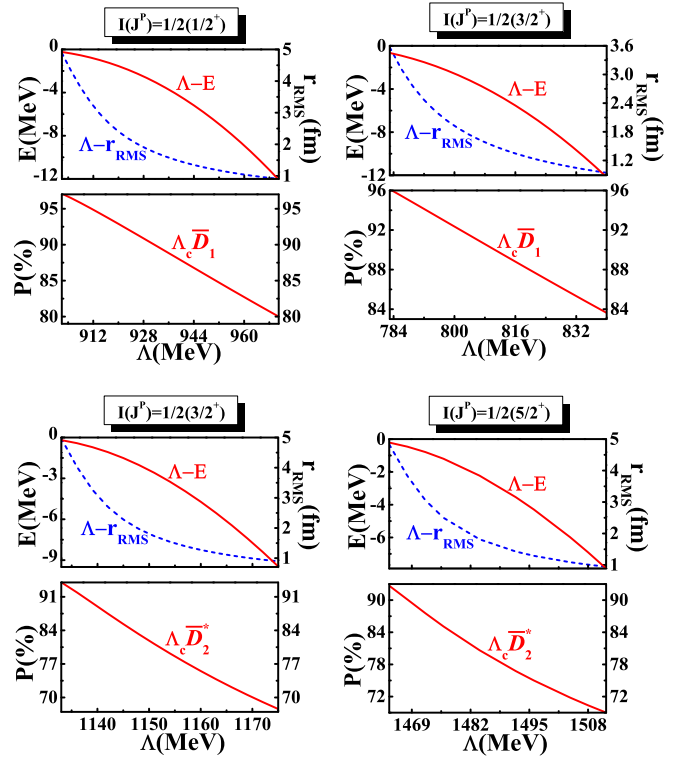

FIG. 2. The cutoff Λ dependence of the binding energy E and root-mean-square radius r_{RMS} for the $\Sigma_c\bar{D}_1$ state with $I(J^P) = 1/2(1/2^+)$ and the $\Sigma_c\bar{D}_2^*$ state with $I(J^P) = 1/2(3/2^+)$ with the OPE model and OBE model, respectively.

FIG. 3. The cutoff Λ dependence of the binding energy E, root-mean-square radius r_{RMS}, and the largest probability P (%) for the $\mathcal{B}_c^{(*)}\bar{T}$ coupled systems with $I(J^P) = 1/2(1/2^+, 3/2^+)$ and $I(J^P) = 1/2(3/2^+, 5/2^+)$; the masses of bound states are defined relative to the $\Lambda_c\bar{D}_1$ and $\Lambda_c\bar{D}_2^*$ thresholds, respectively.

respectively. The specific effective potentials for each component are presented in Appendixes B 1 and B 2. μ_1, μ_2, μ_3, and μ_4 are the reduced masses of the $\Lambda_c\bar{D}_1$, $\Sigma_c\bar{D}_1$, $\Sigma_c^*\bar{D}_1$, and $\Sigma_c^*\bar{D}_2^*$ systems, respectively. In addition, d_i are defined as $d_1 = m_{\Sigma_c} - m_{\Lambda_c}$, $d_2 = m_{\Sigma_c^*} - m_{\Lambda_c}$, and $d_3 = m_{\Sigma_c^*} + m_{D_2^*} - m_{\Lambda_c} - m_{D_1}$. Then, we solve the coupled channel Schrödinger equation and try to find the corresponding bound state solutions.

In Fig. 3, we present the cutoff Λ dependence of the binding energy E, root-mean-square radius r_{RMS}, and the largest probability P (%) for the $\mathcal{B}_c^{(*)}\bar{T}$ coupled systems with $I(J^P) = 1/2(1/2^+, 3/2^+)$ and $I(J^P) = 1/2(3/2^+, 5/2^+)$. The masses of bound states are defined relative to the $\Lambda_c\bar{D}_1$ and $\Lambda_c\bar{D}_2^*$ thresholds, respectively.

After including the coupled channel effects, the bound solutions for the $\mathcal{B}_c^{(*)}\bar{T}$ coupled systems with $I(J^P) = 1/2(1/2^+, 3/2^+)$ and $I(J^P) = 1/2(3/2^+, 5/2^+)$ are obtained when the cutoffs Λ vary in a reasonable range, and they are mainly composed of the $\Lambda_c\bar{D}_1$ channel with probability over 80% and the $\Lambda_c\bar{D}_2^*$ channel with almost 70% probability, respectively. Their RMS radii are around or larger than 1.0 fm, and the binding energies are a few MeV. Therefore, the $\Lambda_c\bar{D}_1$ states with $I(J^P) = 1/2(1/2^+, 3/2^+)$ and $\Lambda_c\bar{D}_2^*$ states with $I(J^P) = 1/2(3/2^+, 5/2^+)$ are possible candidates of the new types of P_c states with the coupled channel effects.

V. DOUBLY CHARMED MOLECULAR PENTAQUARKS

In this work, we extend the obtained OBE effective potentials to search for possible doubly charmed molecular pentaquarks composed of a charmed baryon $\mathcal{B}_c^{(*)} = \Lambda_c/\Sigma_c/\Sigma_c^*$ and an excited charmed meson in a T doublet (D_1, D_2^*), which is an interesting research topic full of opportunities and challenges.

The effective potentials for the doubly charmed $\mathcal{B}_c^{(*)}T$ systems are related to those for hidden-charmed $\mathcal{B}_c^{(*)}\bar{T}$ systems via the G-parity transformation. The potentials induced by the σ, η, and ρ exchanges are same, while those resulting from the π and ω exchanges have opposite signs between the corresponding doubly charmed and hidden-charmed systems with the same isospin and spin-parity quantum numbers [85].

A. $\Sigma_c^{(*)}D_1(D_2^*)$ systems

We show the numerical results for the $\Sigma_c D_1(D_2^*)$ and $\Sigma_c^* D_1(D_2^*)$ systems with the OPE model in Tables VIII and IX, respectively.

In Table VIII, the binding energies and RMS radii are the same for the bound states in the $\Sigma_c D_1$ system with $I(J^P) = 3/2(1/2^+)$ and the $\Sigma_c D_1$ system with $I(J^P) = 1/2(3/2^+)$ when we do not consider the contributions of the D-wave channels, owing to the same product of the matrix elements

TABLE VIII. Bound state properties for the $\Sigma_c^* D_1(D_2^*)$ systems with the OPE model. Conventions are the same as Table III.

$I(J^P)$	Λ	E	r_{RMS}	Λ	E	r_{RMS}	$P\left({}^2\mathbb{S}_{\frac{1}{2}}/{}^4\mathbb{D}_{\frac{1}{2}}\right)$
				$\Sigma_c D_1$			
$\frac{1}{2}\left(\frac{1}{2}^+\right)$				2.62	-0.34	4.68	**95.15**/4.85
				2.78	-3.59	1.80	**85.39**/14.61
				2.94	-12.22	1.08	**75.90**/24.10
$\frac{3}{2}\left(\frac{1}{2}^+\right)$	1.86	-0.26	4.64	1.76	-0.28	4.62	**99.65**/0.35
	2.00	-4.22	1.44	1.90	-3.95	1.52	**99.23**/0.77
	2.13	-12.56	0.87	2.04	-12.46	0.90	**99.05**/0.95
$I(J^P)$	Λ	E	r_{RMS}	Λ	E	r_{RMS}	$P\left({}^4\mathbb{S}_{\frac{3}{2}}/{}^2\mathbb{D}_{\frac{3}{2}}/{}^4\mathbb{D}_{\frac{3}{2}}\right)$
$\frac{1}{2}\left(\frac{3}{2}^+\right)$	1.86	-0.26	4.64	1.22	-0.24	4.96	**97.51**/0.59/1.90
	2.00	-4.22	1.44	1.37	-3.91	1.70	**93.83**/1.45/4.72
	2.13	-12.56	0.87	1.51	-12.25	1.07	**91.85**/1.89/6.26
				$\Sigma_c D_2^*$			
$I(J^P)$	Λ	E	r_{RMS}	Λ	E	r_{RMS}	$P\left({}^4\mathbb{S}_{\frac{3}{2}}/{}^4\mathbb{D}_{\frac{3}{2}}/{}^6\mathbb{D}_{\frac{3}{2}}\right)$
$\frac{1}{2}\left(\frac{3}{2}^+\right)$				2.30	-0.31	4.81	**95.69**/0.94/3.37
				2.50	-3.68	1.83	**87.29**/2.82/9.89
				2.70	-12.83	1.09	**79.66**/4.52/15.82
$\frac{3}{2}\left(\frac{3}{2}^+\right)$	2.03	-0.29	4.51	1.81	-0.20	4.99	**99.42**/0.08/0.50
	2.17	-4.14	1.44	1.96	-3.66	1.58	**98.59**/0.19/1.22
	2.30	-12.10	0.88	2.11	-12.04	0.93	**98.18**/0.25/1.56
$I(J^P)$	Λ	E	r_{RMS}	Λ	E	r_{RMS}	$P\left({}^6\mathbb{S}_{\frac{5}{2}}/{}^4\mathbb{D}_{\frac{5}{2}}/{}^6\mathbb{D}_{\frac{5}{2}}\right)$
$\frac{1}{2}\left(\frac{5}{2}^+\right)$	1.57	-0.20	4.92	1.16	-0.32	4.58	**97.68**/0.95/1.37
	1.70	-3.83	1.52	1.30	-4.05	1.66	**94.95**/2.06/2.99
	1.83	-12.39	0.89	1.43	-12.12	1.05	**93.60**/2.57/3.82

TABLE IX. Bound state properties for the $\Sigma_c^* D_1(D_2^*)$ systems with the OPE model. Conventions are the same as Table III.

System	$I(J^P)$	Λ	E	$r_{\rm RMS}$	Λ	E	$r_{\rm RMS}$	$P\left({}^2\mathbb{S}_{\frac{1}{2}}/{}^4\mathbb{D}_{\frac{1}{2}}/{}^6\mathbb{D}_{\frac{1}{2}}\right)$
	$\frac{1}{2}\left(\frac{1}{2}^+\right)$				1.95	−0.34	4.79	**94.52**/2.57/2.91
					2.13	−3.80	1.85	**83.60**/7.10/9.30
					2.30	−12.72	1.14	**73.93**/10.42/15.65
	$\frac{3}{2}\left(\frac{1}{2}^+\right)$	1.51	−0.20	4.93	1.41	−0.29	4.56	**99.44**/0.34/0.22
		1.64	−3.88	1.51	1.54	−3.88	1.55	**98.83**/0.72/0.45
		1.77	−12.62	0.89	1.67	−12.18	0.94	**98.57**/0.89/0.54
	$I(J^P)$	Λ	E	$r_{\rm RMS}$	Λ	E	$r_{\rm RMS}$	$P\left({}^4\mathbb{S}_{\frac{3}{2}}/{}^2\mathbb{D}_{\frac{3}{2}}/{}^4\mathbb{D}_{\frac{3}{2}}/{}^6\mathbb{D}_{\frac{3}{2}}\right)$
	$\frac{1}{2}\left(\frac{3}{2}^+\right)$				2.10	−0.35	4.62	**95.68**/1.57/2.42/0.33
					2.32	−3.84	1.79	**88.74**/4.15/6.20/0.91
$\Sigma_c^* D_1$					2.54	−12.66	1.11	**83.27**/6.21/9.08/1.44
	$\frac{3}{2}\left(\frac{3}{2}^+\right)$	3.47	−0.21	4.84	2.40	−0.30	4.56	**98.78**/0.31/0.81/0.10
		3.63	−3.98	1.51	2.58	−3.88	1.56	**97.01**/0.75/2.01/0.23
		3.79	−12.55	0.83	2.76	−12.33	0.93	**95.87**/1.03/2.79/0.31
	$I(J^P)$	Λ	E	$r_{\rm RMS}$	Λ	E	$r_{\rm RMS}$	$P\left({}^6\mathbb{S}_{\frac{5}{2}}/{}^2\mathbb{D}_{\frac{5}{2}}/{}^4\mathbb{D}_{\frac{5}{2}}/{}^6\mathbb{D}_{\frac{5}{2}}\right)$
	$\frac{1}{2}\left(\frac{5}{2}^+\right)$	1.30	−0.26	4.63	1.02	−0.22	5.00	**98.10**/0.28/0.08/1.55
		1.42	−3.98	1.51	1.15	−3.77	1.71	**95.62**/0.65/0.17/3.56
		1.54	−12.57	0.91	1.28	−12.53	1.04	**94.42**/0.81/0.22/4.55
	$\frac{3}{2}\left(\frac{5}{2}^+\right)$				3.80	−0.29	4.78	**97.60**/0.10/0.07/2.24
					3.90	−0.99	3.06	**95.95**/0.14/0.12/3.79
					4.00	−2.20	2.14	**94.30**/0.19/0.17/5.34
System	$I(J^P)$	Λ	E	$r_{\rm RMS}$	Λ	E	$r_{\rm RMS}$	$P\left({}^2\mathbb{S}_{\frac{1}{2}}/{}^4\mathbb{D}_{\frac{1}{2}}/{}^6\mathbb{D}_{\frac{1}{2}}\right)$
$\Sigma_c^* D_2^*$	$\frac{1}{2}\left(\frac{1}{2}^+\right)$				1.86	−0.35	4.80	**94.65**/2.37/2.98
					2.06	−3.53	1.95	**85.06**/6.38/8.56
					2.26	−12.10	1.20	**76.58**/9.66/13.76
	$\frac{3}{2}\left(\frac{1}{2}^+\right)$	1.41	−0.27	4.59	1.30	−0.25	4.75	**99.38**/0.32/0.31
		1.54	−4.29	1.44	1.43	−3.85	1.57	**98.64**/0.70/0.66
		1.66	−12.75	0.89	1.56	−12.40	0.94	**98.33**/0.87/0.80
	$I(J^P)$	Λ	E	$r_{\rm RMS}$	Λ	E	$r_{\rm RMS}$	$P\left({}^4\mathbb{S}_{\frac{3}{2}}/{}^2\mathbb{D}_{\frac{3}{2}}/{}^4\mathbb{D}_{\frac{3}{2}}/{}^6\mathbb{D}_{\frac{3}{2}}/{}^8\mathbb{D}_{\frac{3}{2}}\right)$
	$\frac{1}{2}\left(\frac{3}{2}^+\right)$				1.90	−0.27	5.00	**95.31**/1.19/1.56/0.37/1.58
					2.10	−3.64	1.87	**85.84**/3.33/4.30/1.07/5.46
					2.29	−12.50	1.14	**77.75**/4.80/6.17/1.61/9.67
	$\frac{3}{2}\left(\frac{3}{2}^+\right)$	2.00	−0.21	4.85	1.70	−0.21	4.95	**99.17**/0.22/0.39/0.08/0.14
		2.14	−3.82	1.48	1.86	−3.99	1.53	**97.92**/0.55/1.00/0.20/0.34
		2.28	−12.27	0.86	2.01	−12.60	0.91	**97.30**/0.72/1.30/0.25/0.42
	$I(J^P)$	Λ	E	$r_{\rm RMS}$	Λ	E	$r_{\rm RMS}$	$P\left({}^6\mathbb{S}_{\frac{5}{2}}/{}^2\mathbb{D}_{\frac{5}{2}}/{}^4\mathbb{D}_{\frac{5}{2}}/{}^6\mathbb{D}_{\frac{5}{2}}/{}^8\mathbb{D}_{\frac{5}{2}}\right)$
	$\frac{1}{2}\left(\frac{5}{2}^+\right)$				1.80	−0.30	4.76	**96.27**/1.04/0.27/2.33/0.08
					2.01	−3.83	1.76	**90.33**/2.80/0.71/5.94/0.23
					2.21	−12.20	1.10	**86.25**/4.06/1.01/8.35/0.34
	$\frac{3}{2}\left(\frac{5}{2}^+\right)$				2.94	−0.37	4.33	**98.01**/0.22/0.10/1.62/4.68
					3.15	−3.89	1.58	**95.07**/0.50/0.26/4.06/0.11
					3.36	−12.10	0.95	**92.88**/0.68/0.37/5.91/0.16
	$I(J^P)$	Λ	E	$r_{\rm RMS}$	Λ	E	$r_{\rm RMS}$	$P\left({}^8\mathbb{S}_{\frac{7}{2}}/{}^4\mathbb{D}_{\frac{7}{2}}/{}^6\mathbb{D}_{\frac{7}{2}}/{}^8\mathbb{D}_{\frac{7}{2}}\right)$
	$\frac{1}{2}\left(\frac{7}{2}^+\right)$	1.10	−0.21	4.86	0.93	−0.23	4.93	**98.35**/ 0.20/ 0.02/ 1.42
		1.22	−3.64	1.57	1.05	−3.76	1.69	**96.39**/ 0.45/ 0.05/ 3.11
		1.34	−12.62	0.91	1.17	−12.40	1.03	**95.52**/ 0.56/ 0.06/ 3.87
	$\frac{3}{2}\left(\frac{7}{2}^+\right)$				3.65	−0.37	4.45	**97.06**/0.09/0.04/2.81
					3.88	−3.04	1.85	**92.74**/0.18/0.10/6.98
					4.00	−5.77	1.39	**90.66**/0.22/0.13/9.00

TABLE X. Bound state properties for the $\Sigma_c D_1(D_2^*)$ systems with the OBE model. Conventions are the same as Table III.

$I(J^P)$	Λ	E	$r_{\rm RMS}$	Λ	E	$r_{\rm RMS}$	$P(^2\mathbb{S}_{\frac{1}{2}}/^4\mathbb{D}_{\frac{1}{2}})$
				$\Sigma_c D_1$			
$\frac{1}{2}(\frac{1}{2}^+)$	1.31	-0.36	4.81	1.26	-0.32	4.97	**99.20**/0.80
	1.48	-4.53	1.86	1.45	-4.80	1.84	**98.47**/1.53
	1.65	-12.59	1.29	1.63	-12.95	1.29	**98.69**/1.31
$\frac{3}{2}(\frac{1}{2}^+)$	1.38	-0.28	4.70	1.34	-0.24	4.90	**99.82**/0.18
	1.59	-4.24	1.56	1.55	-4.25	1.57	**99.58**/0.42
	1.80	-12.69	0.97	1.75	-12.48	0.99	**99.47**/ 0.53
$I(J^P)$	Λ	E	$r_{\rm RMS}$	Λ	E	$r_{\rm RMS}$	$P(^4\mathbb{S}_{\frac{3}{2}}/^2\mathbb{D}_{\frac{3}{2}}/^4\mathbb{D}_{\frac{3}{2}})$
$\frac{1}{2}(\frac{3}{2}^+)$	0.94	-0.39	4.31	0.91	-0.55	3.92	**98.19**/0.41/1.40
	0.98	-4.72	1.55	0.96	-5.30	1.54	**97.32**/0.59/2.09
	1.01	-11.20	1.09	1.00	-13.35	1.06	**97.49**/0.54/1.97
$\frac{3}{2}(\frac{3}{2}^+)$				3.48	-0.28	4.87	**98.96**/0.17/0.87
				3.79	-1.28	2.78	**98.02**/0.31/1.66
				4.00	-2.48	2.07	**97.39**/0.41/2.20
				$\Sigma_c D_2^*$			
$I(J^P)$	Λ	E	$r_{\rm RMS}$	Λ	E	$r_{\rm RMS}$	$P(^4\mathbb{S}_{\frac{3}{2}}/^4\mathbb{D}_{\frac{3}{2}}/^6\mathbb{D}_{\frac{3}{2}})$
$\frac{1}{2}(\frac{3}{2}^+)$	1.30	-0.40	4.62	1.22	-0.32	4.96	**98.80**/0.24/0.96
	1.47	-4.81	1.80	1.40	-4.47	1.88	**97.65**/0.48/1.88
	1.63	-12.48	1.28	1.58	-12.22	1.31	**97.87**/0.44/1.69
$\frac{3}{2}(\frac{3}{2}^+)$	1.44	-0.23	4.94	1.38	-0.29	4.67	**99.66**/0.05/0.29
	1.67	-4.03	1.59	1.59	-4.06	1.61	**99.25**/0.11/0.64
	1.90	-12.34	0.97	1.80	-12.06	1.00	**99.03**/0.14/0.83
$I(J^P)$	Λ	E	$r_{\rm RMS}$	Λ	E	$r_{\rm RMS}$	$P(^6\mathbb{S}_{\frac{5}{2}}/^4\mathbb{D}_{\frac{5}{2}}/^6\mathbb{D}_{\frac{5}{2}})$
$\frac{1}{2}(\frac{5}{2}^+)$	0.92	-0.45	4.11	0.89	-0.48	4.10	**98.39**/0.64/0.97
	0.96	-5.19	1.47	0.94	-5.34	1.52	**97.58**/0.94/1.48
	0.99	-12.33	1.04	0.98	-13.98	1.03	**97.77**/0.84/1.39
$\frac{3}{2}(\frac{5}{2}^+)$				3.50	-0.29	4.80	**98.81**/0.36/0.83
				3.80	-1.35	2.72	**97.72**/0.69/1.59
				4.00	-2.59	2.03	**96.98**/0.90/2.12

for the operators $\mathcal{A}_2$ and the isospin factors $\mathcal{H}(I)$ giving rise to identical and attractive π exchange interactions. Even if we add the contributions of the S-D wave mixing effects, the bound state solutions are still absent for the $\Sigma_c D_1$ state with $I(J^P) = 3/2(3/2^+)$ and the $\Sigma_c D_2^*$ state with $3/2(5/2^+)$ with the OPE model. From Table IX, we also notice that although the contribution of the π exchange effective potential gives a slightly attractive force for the $\Sigma_c^* D_2^*$ state with $I(J^P) = 3/2(5/2^+)$ when we only consider contributions of the S-wave channel, and we cannot obtain bound state solutions until we increase the cutoffs to be around 4.00 GeV.

We have shown the OPE results above. To compare the properties of the bound states with OPE and OBE models, we still need to present the numerical results with the OBE model. We list the bound state properties of the $\Sigma_c D_1(D_2^*)$ systems and the $\Sigma_c^* D_1(D_2^*)$ systems with the OBE model in Tables X and XI. The exchanges of π, σ, η, ρ, and ω are allowed.

For the $\Sigma_c D_1$ state with $I(J^P) = 1/2(3/2^+)$ and the $\Sigma_c D_2^*$ state with $I(J^P) = 1/2(5/2^+)$, the effective potentials of the σ, π, η, ρ, and ω exchanges all supply attractive forces, and therefore we can obtain loosely bound state solutions with reasonable cutoff values according to the experience of the deuteron [66,67], and thus they can be regarded as good candidates of double-charm molecular pentaquarks. For the $\Sigma_c D_1$ state with $I(J^P) = 1/2(1/2^+)$ and the $\Sigma_c D_2^*$ state with $I(J^P) = 1/2(3/2^+)$, the π exchange potentials provide repulsive forces in the whole range, but the total effective potentials are strongly repulsive in the range from 0.1 to 0.4 fm and slightly attractive in the range $0.4 < r < 1.7$ fm. Our results suggest that there exist bound state solutions with cutoffs around 1.3 GeV as indicated in Table X, and the attractive force that binds these states mainly comes from the ρ and ω exchanges. For the $\Sigma_c D_1$ state with $I(J^P) = 3/2(3/2^+)$ and the $\Sigma_c D_2^*$ state with $I(J^P) = 3/2(5/2^+)$, the π and ρ exchange potentials are repulsive while the σ, η, and ω exchanges provide the attractive force; nevertheless the contributions of

TABLE XI. Bound state properties for the $\Sigma_c^* D_1(D_2^*)$ systems with the OBE model. Conventions are the same as Table III.

System	$I(J^P)$	Λ	E	r_{RMS}	Λ	E	r_{RMS}	$P\left(^2\mathbb{S}_{\frac{1}{2}}/^4\mathbb{D}_{\frac{1}{2}}/^6\mathbb{D}_{\frac{1}{2}}\right)$
	$\frac{1}{2}\left(\frac{1}{2}^+\right)$	1.32	-0.36	4.83	1.22	-0.33	4.97	**98.27**/0.95/0.78
		1.49	-4.50	1.89	1.41	-4.49	1.92	**96.54**/1.91/1.55
		1.65	-12.21	1.33	1.59	-12.15	1.36	**96.81**/1.80/1.39
	$\frac{3}{2}\left(\frac{1}{2}^+\right)$	1.21	-0.23	4.88	1.17	-0.28	4.71	**99.66**/0.20/0.14
		1.38	-4.07	1.58	1.34	-4.36	1.56	**99.28**/0.44/0.28
		1.55	-12.31	0.98	1.50	-12.47	1.00	**99.13**/0.54/0.33
	$I(J^P)$	Λ	E	r_{RMS}	Λ	E	r_{RMS}	$P\left(^4\mathbb{S}_{\frac{3}{2}}/^2\mathbb{D}_{\frac{3}{2}}/^4\mathbb{D}_{\frac{3}{2}}/^6\mathbb{D}_{\frac{3}{2}}\right)$
	$\frac{1}{2}\left(\frac{3}{2}^+\right)$	1.21	-0.33	4.78	1.14	-0.42	4.51	**98.36**/0.56/0.96/0.12
		1.35	-4.83	1.72	1.28	-4.72	1.77	**97.06**/1.01/1.72/0.22
$\Sigma_c^* D_1$		1.49	-12.84	1.20	1.42	-12.06	1.26	**97.17**/0.97/1.65/0.21
	$\frac{3}{2}\left(\frac{3}{2}^+\right)$	1.94	-0.25	4.85	1.68	-0.25	4.90	**99.47**/0.15/0.35/0.04
		2.35	-4.03	1.58	1.99	-4.00	1.63	**98.58**/0.39/0.93/0.11
		2.76	-12.23	0.97	2.29	-12.07	1.01	**97.97**/0.55/1.33/0.15
	$I(J^P)$	Λ	E	r_{RMS}	Λ	E	r_{RMS}	$P\left(^6\mathbb{S}_{\frac{5}{2}}/^2\mathbb{D}_{\frac{5}{2}}/^4\mathbb{D}_{\frac{5}{2}}/^6\mathbb{D}_{\frac{5}{2}}\right)$
	$\frac{1}{2}\left(\frac{5}{2}^+\right)$	0.89	-0.26	4.37	0.86	-0.53	3.93	**98.23**/0.25/0.07/1.45
		0.93	-5.10	1.47	0.90	-4.00	1.70	**97.43**/0.35/0.09/2.12
		0.96	-12.62	1.02	0.94	-11.81	1.10	**97.52**/0.32/0.09/2.07
	$\frac{3}{2}\left(\frac{5}{2}^+\right)$				3.40	-0.29	4.83	**98.60**/0.08/0.04/1.28
					3.70	-1.45	2.63	**97.20**/0.15/0.09/2.57
					4.00	-3.81	1.72	**95.77**/0.20/0.13/3.89
System	$I(J^P)$	Λ	E	r_{RMS}	Λ	E	r_{RMS}	$P\left(^2\mathbb{S}_{\frac{1}{2}}/^4\mathbb{D}_{\frac{1}{2}}/^6\mathbb{D}_{\frac{1}{2}}\right)$
	$\frac{1}{2}\left(\frac{1}{2}^+\right)$	1.32	-0.37	4.80	1.20	-0.34	4.96	**97.88**/1.00/1.11
		1.49	-4.57	1.89	1.39	-4.46	1.94	**95.67**/2.08/2.25
		1.65	-12.45	1.33	1.57	-12.10	1.37	**95.85**/2.03/2.11
	$\frac{3}{2}\left(\frac{1}{2}^+\right)$	1.16	-0.29	4.60	1.10	-0.26	4.78	**99.59**/0.21/0.20
		1.32	-4.35	1.53	1.27	-4.36	1.56	**99.13**/0.44/0.43
		1.47	-12.20	0.98	1.42	-12.51	1.00	**98.95**/0.54/0.51
	$I(J^P)$	Λ	E	r_{RMS}	Λ	E	r_{RMS}	$P\left(^4\mathbb{S}_{\frac{3}{2}}/^2\mathbb{D}_{\frac{3}{2}}/^4\mathbb{D}_{\frac{3}{2}}/^6\mathbb{D}_{\frac{3}{2}}/^8\mathbb{D}_{\frac{3}{2}}\right)$
	$\frac{1}{2}\left(\frac{3}{2}^+\right)$	1.29	-0.34	4.82	1.18	-0.33	4.90	**98.09**/0.54/0.74/0.16/0.48
		1.46	-4.65	1.81	1.37	-4.78	1.83	**96.14**/1.10/1.48/0.31/0.97
		1.63	-12.88	1.26	1.55	-12.47	1.30	**96.37**/1.07/1.42/0.29/0.86
	$\frac{3}{2}\left(\frac{3}{2}^+\right)$	1.43	-0.27	4.70	1.33	-0.26	4.78	**99.51**/0.13/0.22/0.05/0.09
		1.66	-4.28	1.53	1.54	-4.18	1.58	**98.86**/0.31/0.53/0.11/0.20
$\Sigma_c^* D_2^*$		1.88	-12.39	0.96	1.74	-12.20	0.99	**98.53**/0.40/0.69/0.14/0.25
	$I(J^P)$	Λ	E	r_{RMS}	Λ	E	r_{RMS}	$P\left(^6\mathbb{S}_{\frac{5}{2}}/^2\mathbb{D}_{\frac{5}{2}}/^4\mathbb{D}_{\frac{5}{2}}/^6\mathbb{D}_{\frac{5}{2}}/^8\mathbb{D}_{\frac{5}{2}}\right)$
	$\frac{1}{2}\left(\frac{5}{2}^+\right)$	1.10	-0.38	4.49	1.04	-0.36	4.60	**98.33**/0.41/0.11/1.11/0.03
		1.18	-4.77	1.63	1.13	-4.65	1.70	**97.00**/0.73/0.20/1.99/0.07
		1.25	-11.96	1.13	1.21	-12.08	1.17	**97.07**/0.70/0.19/1.96/0.07
	$\frac{3}{2}\left(\frac{5}{2}^+\right)$	3.50	-0.31	4.61	2.07	-0.26	4.85	**99.18**/0.12/0.05/0.64/0.02
		3.80	-0.71	3.43	2.49	-3.83	1.66	**97.66**/0.32/0.13/1.84/0.05
		4.00	-1.05	2.90	2.91	-11.45	1.03	**96.48**/0.46/0.19/2.79/0.08
	$I(J^P)$	Λ	E	r_{RMS}	Λ	E	r_{RMS}	$P\left(^8\mathbb{S}_{\frac{7}{2}}/^4\mathbb{D}_{\frac{7}{2}}/^6\mathbb{D}_{\frac{7}{2}}/^8\mathbb{D}_{\frac{7}{2}}\right)$
	$\frac{1}{2}\left(\frac{7}{2}^+\right)$	0.86	-0.27	4.69	0.83	-0.47	4.06	**98.36**/0.19/0.02/1.42
		0.90	-4.68	1.50	0.88	-5.04	1.53	**97.52**/0.29/0.03/2.16
		0.93	-12.09	1.02	0.92	-13.93	1.01	**97.67**/0.26/0.03/2.04
	$\frac{3}{2}\left(\frac{7}{2}^+\right)$				3.40	-0.34	4.62	**98.32**/0.07/0.02/1.59
					3.70	-1.66	2.48	**96.62**/0.13/0.05/3.20
					4.00	-4.36	1.62	**94.89**/0.18/0.07/4.85

TABLE XII. Ratings for predicted double-charm molecular pentaquarks with $\Sigma_c^{(*)}D_1(D_2^*)$ systems (I, J).

Rating	$\Sigma_c D_1$	$\Sigma_c D_2^*$	$\Sigma_c^* D_1$	$\Sigma_c^* D_2^*$
★★★★		$\left(\frac{1}{2}, \frac{5}{2}\right)$	$\left(\frac{1}{2}, \frac{5}{2}\right), \left(\frac{3}{2}, \frac{1}{2}\right)$	$\left(\frac{1}{2}, \frac{7}{2}\right), \left(\frac{3}{2}, \frac{1}{2}\right)$
★★★	$\left(\frac{1}{2}, \frac{3}{2}\right)$			
★★	$\left(\frac{1}{2}/\frac{3}{2}, \frac{1}{2}\right)$	$\left(\frac{1}{2}/\frac{3}{2}, \frac{3}{2}\right)$	$\left(\frac{1}{2}, \frac{1}{2}/\frac{3}{2}\right)$	$\left(\frac{1}{2}, \frac{1}{2}/\frac{3}{2}/\frac{5}{2}\right), \left(\frac{3}{2}, \frac{3}{2}\right)$
★				

the ρ and ω exchanges cancel each other almost exactly, and thus the total effective potentials are repulsive in the whole range and dominated by the π exchange potentials. In most cases of the $\Sigma_c D_1(D_2^*)$ systems and the $\Sigma_c^* D_1(D_2^*)$ systems, if we take the same cutoff parameters, it is clear that the numerical results within the OBE model are similar to those within the OPE model except that the bindings become deeper.

From Tables X and XI, we notice there are some similarities between the $\Sigma_c D_1(D_2^*)$. For instance, in the $\Sigma_c^* D_1$ system with $I(J^P) = 1/2(1/2^+, 3/2^+)$ and the $\Sigma_c^* D_2^*$ system with $I(J^P) = 1/2(1/2^+, 3/2^+, 5/2^+)$, the bound states can also be obtained with cutoff parameters of about 1.3 GeV.

Compared with the results with the OPE model in Table IX, the $\Sigma_c^* D_1(D_2^*)$ states with the OBE model are more likely to be bound in many of the cases from Table XI. The main reason is that the σ exchange interaction always provides an attractive force, and the vector meson exchange effective potential usually plays an essential role in forming the loosely bound molecular states for many of the $\Sigma_c^* D_1(D_2^*)$ states.

To summarize, we can predict a series of possible candidates of double-charm molecular pentaquarks with the structures of $\Sigma_c^{(*)}T$ as shown in Tables IX–XI. If we use the same criteria as the $\Sigma_c^{(*)}\bar{T}$-type hidden-charm molecular pentaquarks, we can also present the ratings for these double-charm molecular pentaquarks in Table XII, which provides crucial information for further experimental search. According to our calculations, we find that there exist ideal candidates of the double-charm molecular pentaquarks, such as the $\Sigma_c D_2^*$ state with $I(J^P) = 1/2(5/2^+)$, the $\Sigma_c^* D_1$ states with $I(J^P) = 1/2(5/2^+), 3/2(1/2^+)$, and the $\Sigma_c^* \bar{D}_2^*$ states with $I(J^P) = 1/2(7/2^+), 3/2(1/2^+)$.

B. $\Lambda_c D_1(D_2^*)$ systems

We also extend our work to investigate the bound properties of the $\Lambda_c D_1(D_2^*)$ systems. Similarly to the $\Lambda_c \bar{D}_1(\bar{D}_2^*)$ systems, we also mainly focus on the results of the coupled channel effects in forming these bound states within the OBE model. For the $\Lambda_c D_1(D_2^*)$ systems, only the σ and ω exchanges are allowed and both provide attractive potentials. They enhance each other and lead to a strong interaction. By solving the coupled channel Schrödinger equation, we can obtain bound solutions for the $\Lambda_c D_1$ states with $I(J^P) = 1/2(1/2^+, 3/2^+)$ and for the $\Lambda_c D_2^*$ states with $I(J^P) = 1/2(3/2^+, 5/2^+)$; the corresponding numerical results are presetnted in Table XIII. Thus, we conclude that these four states are possible candidates of double-charm molecular pentaquarks with coupled channel effects.

TABLE XIII. Bound state properties for the $\Lambda_c D_1(D_2^*)$ systems. Conventions are the same as Table III.

Systems	Λ	E	r_{RMS}	Λ	E	r_{RMS}
	$(J = 1/2, I = 1/2)$			$(J = 3/2, I = 1/2)$		
$\Lambda_c D_1$	0.96	−0.45	4.15	0.82	−0.30	4.63
	1.00	−4.30	1.56	0.86	−4.40	1.52
	1.04	−12.25	0.98	0.90	−12.96	0.94
	$(J = 3/2, I = 1/2)$			$(J = 5/2, I = 1/2)$		
$\Lambda_c D_2^*$	1.07	−0.59	3.73	1.09	−0.24	4.94
	1.09	−5.03	1.31	1.11	−4.24	1.42
	1.10	−10.44	0.86	1.12	−12.00	0.73

VI. SUMMARY

Very recently, the LHCb Collaboration updated the observations of P_c states by analyzing $\Lambda_b^0 \to J/\psi p K^-$. They not only reported a new structure, $P_c(4312)$, but also found that the $P_c(4450)$ previously reported consist of two narrow overlapping peaks, $P_c(4440)$ and $P_c(4457)$ [7]. These P_c states can be naturally interpreted as hidden-charm molecular pentaquarks composed of an S-wave charmed baryon and an S-wave anticharmed meson since the masses of the three P_c states are just below the $\Sigma_c \bar{D}^{(*)}$ thresholds [30].

In this work, we try to search for possible new types of P_c states composed of an S-wave charmed baryon and an anti charmed meson in a T doublet with the structures of $\mathcal{B}_c^{(*)}\bar{T}$. In the present study, both the S-D wave mixing effects and the coupled channel effects are taken into consideration. As for the unknown coupling constants, we estimate them within the quark model. Our results indicate that there exist ideal candidates of new types of P_c states: the $\Sigma_c \bar{D}_1$ state with $I(J^P) = 1/2(1/2^+)$, the $\Sigma_c \bar{D}_2^*$ state with $I(J^P) = 1/2(3/2^+)$, the $\Sigma_c^* \bar{D}_1$ state with $I(J^P) = 1/2(1/2^+)$, and the $\Sigma_c^* \bar{D}_2^*$ states with $I(J^P) = 1/2(1/2^+, 3/2^+)$. Moreover, the low spin $\Sigma_c^{(*)}\bar{T}$ states with $I = 1/2$ configuration can be more stable than the $I = 3/2$ states with the same spin-parity configuration, and we also find that the coupled channel effects play an essential role for the $\Lambda_c \bar{T}$ systems; especially the $\Lambda_c \bar{D}_1$ states with $I(J^P) = 1/2(1/2^+, 3/2^+)$ and $\Lambda_c \bar{D}_2^*$ states with $I(J^P) = 1/2(3/2^+, 5/2^+)$ disappear without considering the coupled channel effects. Besides the above predictions, we extend our study to the interactions between an S-wave ground charmed baryon and a charmed meson in a T doublet, and can predict the existence of double-charm molecular pentaquarks with typical quark configuration $ccq\bar{q}$.

Experimental searches for these predicted new types of P_c states are an interesting research topic. Obviously, we suggest that the Λ_b baryon decay is an ideal process to produce these predicted new type of P_c states, which can decay into a ground charmed baryon with a ground anticharmed meson, and a charmonium with a light baryon if kinetically allowed, like $\Lambda_c \bar{D}^{(*)}$, $\Sigma_c^{(*)} \bar{D}^{(*)}$, $\eta_c(nS)N/\Delta$ ($n \leqslant 2$), $\psi(nS)N/\Delta$ ($n \leqslant 2$), $\chi_{cJ}(1P)N/\Delta$ ($J \leqslant 2$). Experimental searches for these possible new types of P_c states can be also a crucial test of hadronic molecular state assignments to the P_c states. The P_c states are observed in the $\Lambda_b^0 \to J/\psi p \pi^-$ process by the

LHCb Collaboration [7], and thus it would provide a sign for the success of our work if these predicted states are detected in the process $\Lambda_b^0 \to \psi(2S)p\pi^-$ since these and P_c states have similar structures in the molecule picture. Actually, the decay $\Lambda_b^0 \to \psi(2S)p\pi^-$ has been reported in the search for hidden-charm pentaquark states with higher mass by the LHCb experiment [86]. Unfortunately, no significant exotic pentaquarks are observed due to the bin size of experimental events being a little large. As commonly believed, a resonance could not be identified in such rough data, especially a narrow resonance. Thus, we hope further experiments can provide a more precise measurement of the process $\Lambda_b^0 \to \psi(2S)p\pi^-$, and the existence of more P_c states with larger mass should be revealed in the $\psi(2S)p$ invariant mass spectrum, especially for the low spin $\Sigma_c^{(*)}\bar{D}_1(\bar{D}_2^*)$ with $I = 1/2$ states.

The possible doubly charmed molecular pentaquarks with the structures of $\mathcal{B}_c^{(*)}T$ can be searched for in their possible two-body strong decay channels

$$\Lambda_c D^{(*)}, \quad \Sigma_c^{(*)}D^{(*)}, \quad \Xi_{cc}\pi, \quad \Xi_{cc}\rho, \quad \Xi_{cc}\omega, \quad \Xi_{cc}\eta^{(\prime)},$$

which helps to further explore them in experiments. These doubly charmed molecular pentaquarks may be produced via proton-proton collisions, and we hope experimental colleagues will bring us more surprises after the LHCb observations of three P_c states [7]. Nevertheless, we notice that no open-charm multiquark states have been reported up to now. Experimental searched for these possible doubly charmed molecular pentaquarks are still difficult compared with the hidden-charm exotic hadronic states.

Since 2003, the observations of abundant charmoniumlike XYZ states have stimulated extensive discussion of the interactions between charmed mesons and anticharmed mesons [1]. With the observation of three P_c states by LHCb, searching for heavy flavor pentaquarks will become a hot topic of hadron physics; more opportunities and challenges are waiting for us. Different from P_c states composed of an S-wave charmed baryon and an S-wave anticharmed meson [32], we find that new types of P_c states with the structures of $\mathcal{B}_c^{(*)}\bar{T}$ are more abundant due to different quantum number configurations, and we have reason to believe that these predicted new types of P_c states can be accessible in future experiments in the next decades.

APPENDIX A: THE DETAILED LAGRANGIANS

The detailed effective Lagrangians for anticharmed mesons in a $\bar{T}$ doublet and light mesons are expressed as

$$\mathcal{L}_{\bar{T}\bar{T}\sigma} = -2g''_\sigma \bar{D}_{1a\mu}\bar{D}_{1a}^{\mu\dagger}\sigma + 2g''_\sigma \bar{D}_{2a\mu\nu}^{*\dagger}\bar{D}_{2a}^{*\mu\nu}\sigma, \tag{A1}$$

$$\mathcal{L}_{\bar{T}\bar{T}\mathbb{P}} = -\frac{5ik}{3f_\pi}\varepsilon^{\mu\nu\rho\tau}v_\nu\bar{D}_{1a\rho}^\dagger\bar{D}_{1b\tau}\partial_\mu\mathbb{P}_{ba} + \frac{2ik}{f_\pi}\varepsilon^{\mu\nu\rho\tau}v_\nu\bar{D}_{2a\rho}^{*\alpha\dagger}\bar{D}_{2b\alpha\tau}^*\partial_\mu\mathbb{P}_{ba} + \sqrt{\frac{2}{3}}\frac{k}{f_\pi}\left(\bar{D}_{1a\mu}^\dagger\bar{D}_{2b}^{*\mu\lambda} + \bar{D}_{1b\mu}\bar{D}_{2a}^{*\mu\lambda\dagger}\right)\partial_\lambda\mathbb{P}_{ba}, \tag{A2}$$

$$\begin{aligned}
\mathcal{L}_{\bar{T}\bar{T}\mathbb{V}} = {}& \sqrt{2}\beta''g_V(v\cdot\mathbb{V}_{ba})\bar{D}_{1b\mu}\bar{D}_{1a}^{\mu\dagger} + \frac{5\sqrt{2}i\lambda''g_V}{3}\left(\bar{D}_{1b}^\nu\bar{D}_{1a}^{\mu\dagger} - \bar{D}_{1a}^{\nu\dagger}\bar{D}_{1b}^\mu\right)\partial_\mu\mathbb{V}_{bav} \\
& - \sqrt{2}\beta''g_V(v\cdot\mathbb{V}_{ba})\bar{D}_{2b}^{*\lambda\nu}\bar{D}_{2a\lambda\nu}^{*\dagger} + 2\sqrt{2}i\lambda''g_V\left(\bar{D}_{2a}^{*\lambda\nu\dagger}\bar{D}_{2b\lambda}^{*\mu} - \bar{D}_{2b}^{*\lambda\nu}\bar{D}_{2a\lambda}^{*\mu\dagger}\right)\partial_\mu\mathbb{V}_{bav} \\
& + \frac{i\beta''g_V}{\sqrt{3}}\varepsilon^{\lambda\alpha\rho\tau}v_\rho(v\cdot\mathbb{V}_{ba})(\bar{D}_{1a\alpha}^\dagger\bar{D}_{2b\lambda\tau}^* - \bar{D}_{1b\alpha}\bar{D}_{2a\lambda\tau}^{*\dagger}) + \frac{2\lambda''g_V}{\sqrt{3}}\Big[3\varepsilon^{\mu\lambda\nu\tau}v_\lambda\left(\bar{D}_{1a}^{\alpha\dagger}\bar{D}_{2b\alpha\tau}^* + \bar{D}_{1b}^\alpha\bar{D}_{2a\alpha\tau}^{*\dagger}\right)\partial_\mu\mathbb{V}_{bav} \\
& + 2\varepsilon^{\lambda\alpha\rho\nu}v_\rho\left(\bar{D}_{1a\alpha}^\dagger\bar{D}_{2b\lambda}^{*\mu} + \bar{D}_{1b\alpha}\bar{D}_{2a\lambda}^{\dagger\mu*}\right)(\partial_\mu\mathbb{V}_{bav} - \partial_\nu\mathbb{V}_{ba\mu})\Big],
\end{aligned} \tag{A3}$$

and those for S-wave charmed baryons and light mesons are

$$\mathcal{L}_{\mathcal{B}_{\bar{3}}\mathcal{B}_{\bar{3}}\sigma} = l_B\langle\bar{\mathcal{B}}_{\bar{3}}\sigma\mathcal{B}_{\bar{3}}\rangle, \tag{A4}$$

$$\mathcal{L}_{\mathcal{B}_{\bar{3}}\mathcal{B}_{\bar{3}}\mathbb{V}} = \frac{1}{\sqrt{2}}\beta_B g_V\langle\bar{\mathcal{B}}_{\bar{3}}v\cdot\mathbb{V}\mathcal{B}_{\bar{3}}\rangle, \tag{A5}$$

$$\mathcal{L}_{\mathcal{B}_6^{(*)}\mathcal{B}_6^{(*)}\sigma} = -l_S\langle\bar{\mathcal{B}}_6\sigma\mathcal{B}_6\rangle + l_S\langle\bar{\mathcal{B}}_{6\mu}^*\sigma\mathcal{B}_6^{*\mu}\rangle - \frac{l_S}{\sqrt{3}}\langle\bar{\mathcal{B}}_{6\mu}^*\sigma(\gamma^\mu + v^\mu)\gamma^5\mathcal{B}_6\rangle + \text{H.c.}, \tag{A6}$$

$$\mathcal{L}_{\mathcal{B}_6^{(*)}\mathcal{B}_6^{(*)}\mathbb{P}} = i\frac{g_1}{2f_\pi}\varepsilon^{\mu\nu\lambda\kappa}v_\kappa\langle\bar{\mathcal{B}}_6\gamma_\mu\gamma_\lambda\partial_\nu\mathbb{P}\mathcal{B}_6\rangle + i\frac{\sqrt{3}g_1}{2f_\pi}v_\kappa\varepsilon^{\mu\nu\lambda\kappa}\langle\bar{\mathcal{B}}_{6\mu}^*\partial_\nu\mathbb{P}\gamma_\lambda\gamma^5\mathcal{B}_6\rangle + \text{H.c.} - i\frac{3g_1}{2f_\pi}\varepsilon^{\mu\nu\lambda\kappa}v_\kappa\langle\bar{\mathcal{B}}_{6\mu}^*\partial_\nu\mathbb{P}\mathcal{B}_{6\lambda}^*\rangle, \tag{A7}$$

$$\mathcal{L}_{\mathcal{B}_6^{(*)}\mathcal{B}_6^{(*)}\mathbb{V}} = -\frac{\beta_S g_V}{\sqrt{2}}\langle\bar{\mathcal{B}}_6 v\cdot\mathbb{V}\mathcal{B}_6\rangle + \frac{\beta_S g_V}{\sqrt{2}}\langle\bar{\mathcal{B}}_{6\mu}^* v\cdot V\mathcal{B}_6^{*\mu}\rangle - i\frac{\lambda_S g_V}{3\sqrt{2}}\langle\bar{\mathcal{B}}_6\gamma_\mu\gamma_\nu(\partial^\mu\mathbb{V}^\nu - \partial^\nu\mathbb{V}^\mu)\mathcal{B}_6\rangle + i\frac{\lambda_S g_V}{\sqrt{2}}\langle\bar{\mathcal{B}}_{6\mu}^*(\partial^\mu\mathbb{V}^\nu - \partial^\nu\mathbb{V}^\mu)\mathcal{B}_{6\nu}^*\rangle$$

$$+ \text{H.c.} - i\frac{\lambda_S g_V}{\sqrt{6}}\langle\bar{\mathcal{B}}_{6\mu}^*(\partial^\mu\mathbb{V}^\nu - \partial^\nu\mathbb{V}^\mu)(\gamma_\nu + v_\nu)\gamma^5\mathcal{B}_6\rangle - \frac{\beta_S g_V}{\sqrt{6}}\langle\bar{\mathcal{B}}_{6\mu}^* v\cdot\mathbb{V}(\gamma^\mu + v^\mu)\gamma^5\mathcal{B}_6\rangle, \tag{A8}$$

$$\mathcal{L}_{\mathcal{B}_{\bar{3}}\mathcal{B}_6^{(*)}\mathbb{P}} = -\sqrt{\frac{1}{3}}\frac{g_4}{f_\pi}\langle\bar{\mathcal{B}}_6\gamma^5(\gamma^\mu + v^\mu)\partial_\mu\mathbb{P}\mathcal{B}_{\bar{3}}\rangle - \frac{g_4}{f_\pi}\langle\bar{\mathcal{B}}_{6\mu}^*\partial^\mu\mathbb{P}\mathcal{B}_{\bar{3}}\rangle + \text{H.c.}, \tag{A9}$$

$$\mathcal{L}_{\mathcal{B}_3\mathcal{B}_6^{(*)}\mathbb{V}} = -\frac{\lambda_I g_V}{\sqrt{2}}\varepsilon^{\mu\nu\lambda\kappa}v_\mu\langle\bar{\mathcal{B}}_{6\nu}^*(\partial_\lambda\mathbb{V}_\kappa - \partial_\kappa\mathbb{V}_\lambda)\mathcal{B}_{\bar{3}}\rangle + \text{H.c.} - \frac{\lambda_I g_V}{\sqrt{6}}\varepsilon^{\mu\nu\lambda\kappa}v_\mu\langle\bar{\mathcal{B}}_6\gamma^5\gamma_\nu(\partial_\lambda\mathbb{V}_\kappa - \partial_\kappa\mathbb{V}_\lambda)\mathcal{B}_{\bar{3}}\rangle. \tag{A10}$$

APPENDIX B: RELEVANT SUBPOTENTIALS

For convenience, we define the following functions:

$$\mathcal{H}(I = 1/2)Y(\Lambda, m_P, r) = -Y(\Lambda, m_\pi, r) + \frac{1}{6}Y(\Lambda, m_\eta, r),$$

$$\mathcal{G}(I = 1/2)Y(\Lambda, m_V, r) = -Y(\Lambda, m_\rho, r) + \frac{1}{2}Y(\Lambda, m_\omega, r),$$

$$\mathcal{H}(I = 3/2)Y(\Lambda, m_P, r) = \frac{1}{2}Y(\Lambda, m_\pi, r) + \frac{1}{6}Y(\Lambda, m_\eta, r),$$

$$\mathcal{G}(I = 3/2)Y(\Lambda, m_V, r) = \frac{1}{2}Y(\Lambda, m_\rho, r) + \frac{1}{2}Y(\Lambda, m_\omega, r),$$

$$Y_E \equiv Y(\Lambda, m_E, r) = \frac{1}{4\pi r}(e^{-m_E r} - e^{-\Lambda r}) - \frac{\Lambda^2 - m_E^2}{8\pi\Lambda}e^{-\Lambda r}, \tag{B1}$$

respectively. Here, $\mathcal{H}(I)$ and $\mathcal{G}(I)$ are the isospin factors for the $\Sigma_c^{(*)}\bar{D}_1(\bar{D}_2^*)$ systems, and I denotes the isospin. Additionally, we also define several variables: $A = l_B g_\sigma''$, $B = \beta_B\beta'' g_V^2$, $C = l_S g_\sigma''$, $D = g_1 k/f_\pi^2$, $E = \beta_S\beta'' g_V^2$, $F = \lambda_S\lambda'' g_V^2$, $G = g_4 k/f_\pi^2$, and $H = \lambda_I\lambda'' g_V^2$.

1. The effective potentials involved in $\Sigma_c^{(*)}\bar{D}_1(\bar{D}_2^*)$ systems

With the above preparation, the OBE effective potentials in the analysis of the $\Sigma_c^{(*)}\bar{D}_1(\bar{D}_2^*)$ systems are given by

$$\mathcal{V}^{\Sigma_c\bar{D}_1\to\Sigma_c\bar{D}_1}(\mathbf{r}) = CY_\sigma\mathcal{A}_1 + \frac{1}{2}E\mathcal{G}(I)Y_V\mathcal{A}_1 + \frac{5}{18}D\mathcal{H}(I)\left[\mathcal{A}_2\nabla^2 + \mathcal{A}_3 r\frac{\partial}{\partial r}\frac{1}{r}\frac{\partial}{\partial r}\right]Y_P - \frac{5}{27}F\mathcal{G}(I)\left[2\mathcal{A}_2\nabla^2 - \mathcal{A}_3 r\frac{\partial}{\partial r}\frac{1}{r}\frac{\partial}{\partial r}\right]Y_V, \tag{B2}$$

$$\mathcal{V}^{\Sigma_c\bar{D}_2^*\to\Sigma_c\bar{D}_2^*}(\mathbf{r}) = CY_\sigma\mathcal{A}_4 + \frac{1}{2}E\mathcal{G}(I)Y_V\mathcal{A}_4 + \frac{1}{3}D\mathcal{H}(I)\left[\mathcal{A}_5\nabla^2 + \mathcal{A}_6 r\frac{\partial}{\partial r}\frac{1}{r}\frac{\partial}{\partial r}\right]Y_P - \frac{2}{9}F\mathcal{G}(I)\left[2\mathcal{A}_5\nabla^2 - \mathcal{A}_6 r\frac{\partial}{\partial r}\frac{1}{r}\frac{\partial}{\partial r}\right]Y_V, \tag{B3}$$

$$\mathcal{V}^{\Sigma_c^*\bar{D}_1\to\Sigma_c^*\bar{D}_1}(\mathbf{r}) = CY_\sigma\mathcal{A}_7 + \frac{1}{2}E\mathcal{G}(I)Y_V\mathcal{A}_7 + \frac{5}{12}D\mathcal{H}(I)\left[\mathcal{A}_8\nabla^2 + \mathcal{A}_9 r\frac{\partial}{\partial r}\frac{1}{r}\frac{\partial}{\partial r}\right]Y_P - \frac{5}{18}F\mathcal{G}(I)\left[2\mathcal{A}_8\nabla^2 - \mathcal{A}_9 r\frac{\partial}{\partial r}\frac{1}{r}\frac{\partial}{\partial r}\right]Y_V, \tag{B4}$$

$$\mathcal{V}^{\Sigma_c^*\bar{D}_2^*\to\Sigma_c^*\bar{D}_2^*}(\mathbf{r}) = CY_\sigma\mathcal{A}_{10} + \frac{1}{2}E\mathcal{G}(I)Y_V\mathcal{A}_{10} + \frac{1}{2}D\mathcal{H}(I)\left[\mathcal{A}_{11}\nabla^2 + \mathcal{A}_{12} r\frac{\partial}{\partial r}\frac{1}{r}\frac{\partial}{\partial r}\right]Y_P - \frac{1}{3}F\mathcal{G}(I)\left[2\mathcal{A}_{11}\nabla^2 - \mathcal{A}_{12} r\frac{\partial}{\partial r}\frac{1}{r}\frac{\partial}{\partial r}\right]Y_V. \tag{B5}$$

In Eqs. (B2)–(B5), we define several operators, i.e.,

$$\mathcal{A}_1 = \boldsymbol{\epsilon}_4^\dagger\cdot\boldsymbol{\epsilon}_2\chi_3^\dagger\chi_1,$$

$$\mathcal{A}_2 = \chi_3^\dagger[\boldsymbol{\sigma}\cdot(i\boldsymbol{\epsilon}_4^\dagger\times\boldsymbol{\epsilon}_2)]\chi_1,$$

$$\mathcal{A}_3 = \chi_3^\dagger S(\boldsymbol{\sigma}, i\boldsymbol{\epsilon}_4^\dagger\times\boldsymbol{\epsilon}_2, \hat{\boldsymbol{r}})\chi_1,$$

$$\mathcal{A}_4 = \mathcal{X}\mathcal{Y}(\boldsymbol{\epsilon}_{4m}^\dagger\cdot\boldsymbol{\epsilon}_{2a})(\boldsymbol{\epsilon}_{4n}^\dagger\cdot\boldsymbol{\epsilon}_{2b})\chi_3^\dagger\chi_1,$$

$$\mathcal{A}_5 = \mathcal{X}\mathcal{Y}(\boldsymbol{\epsilon}_{4m}^\dagger\cdot\boldsymbol{\epsilon}_{2a})\chi_3^\dagger[\boldsymbol{\sigma}\cdot(i\boldsymbol{\epsilon}_{4n}^\dagger\times\boldsymbol{\epsilon}_{2b})]\chi_1,$$

TABLE XIV. Matrix elements $\langle f|\mathcal{A}_k|i\rangle$ in various channels for operators $\mathcal{A}_k$ in the effective potentials.

Spin	$J=1/2$	$J=3/2$	$J=5/2$	$J=7/2$
$\langle\mathcal{A}_{1}\rangle$	$\mathrm{diag}(1,1)$	$\mathrm{diag}(1,1,1)$		
$\langle\mathcal{A}_{2}\rangle$	$\mathrm{diag}(2,-1)$	$\mathrm{diag}(-1,2,-1)$		
$\langle\mathcal{A}_{3}\rangle$	$\begin{pmatrix} 0 & \sqrt{2} \\ \sqrt{2} & 2 \end{pmatrix}$	$\begin{pmatrix} 0 & -1 & -2 \\ -1 & 0 & 1 \\ -2 & 1 & 0 \end{pmatrix}$		
$\langle\mathcal{A}_{4}\rangle$		$\mathrm{diag}(1,1,1)$	$\mathrm{diag}(1,1,1)$	
$\langle\mathcal{A}_{5}\rangle$		$\mathrm{diag}\left(\tfrac{3}{2},\tfrac{3}{2},-1\right)$	$\mathrm{diag}\left(-1,\tfrac{3}{2},-1\right)$	
$\langle\mathcal{A}_{6}\rangle$		$\begin{pmatrix} 0 & \frac{3}{5} & \frac{3\sqrt{21}}{10} \\ \frac{3}{5} & 0 & \frac{3\sqrt{21}}{14} \\ \frac{3\sqrt{21}}{10} & \frac{3\sqrt{21}}{14} & \frac{4}{7} \end{pmatrix}$	$\begin{pmatrix} 0 & -\frac{3\sqrt{14}}{10} & -\frac{2\sqrt{14}}{5} \\ -\frac{3\sqrt{14}}{10} & \frac{3}{7} & \frac{3}{7} \\ -\frac{2\sqrt{14}}{5} & \frac{3}{7} & -\frac{4}{7} \end{pmatrix}$	
$\langle\mathcal{A}_{7}\rangle$	$\mathrm{diag}(1,1,1)$	$\mathrm{diag}(1,1,1,1)$	$\mathrm{diag}(1,1,1,1)$	
$\langle\mathcal{A}_{8}\rangle$	$\mathrm{diag}\left(\tfrac{5}{3},\tfrac{2}{3},-1\right)$	$\mathrm{diag}\left(\tfrac{2}{3},\tfrac{5}{3},\tfrac{2}{3},-1\right)$	$\mathrm{diag}\left(-1,\tfrac{5}{3},\tfrac{2}{3},-1\right)$	
$\langle\mathcal{A}_{9}\rangle$	$\begin{pmatrix} 0 & -\frac{7}{3\sqrt{5}} & \frac{2}{\sqrt{5}} \\ -\frac{7}{3\sqrt{5}} & \frac{16}{15} & -\frac{1}{5} \\ \frac{2}{\sqrt{5}} & -\frac{1}{5} & \frac{8}{5} \end{pmatrix}$	$\begin{pmatrix} 0 & \frac{7}{3\sqrt{10}} & -\frac{16}{15} & -\frac{\sqrt{7}}{5\sqrt{2}} \\ \frac{7}{3\sqrt{10}} & 0 & \frac{7}{3\sqrt{10}} & -\frac{\sqrt{2}}{\sqrt{35}} \\ -\frac{16}{15} & \frac{7}{3\sqrt{10}} & 0 & -\frac{1}{\sqrt{14}} \\ -\frac{\sqrt{7}}{5\sqrt{2}} & -\frac{2}{\sqrt{35}} & -\frac{1}{\sqrt{14}} & \frac{4}{7} \end{pmatrix}$	$\begin{pmatrix} 0 & \frac{2}{\sqrt{15}} & \frac{\sqrt{7}}{5\sqrt{3}} & -\frac{2\sqrt{14}}{5} \\ \frac{2}{\sqrt{15}} & 0 & \frac{\sqrt{7}}{3\sqrt{5}} & -\frac{4\sqrt{2}}{\sqrt{105}} \\ \frac{\sqrt{7}}{5\sqrt{3}} & \frac{\sqrt{7}}{3\sqrt{5}} & -\frac{16}{21} & -\frac{\sqrt{2}}{7\sqrt{3}} \\ -\frac{2\sqrt{14}}{5} & -\frac{4\sqrt{2}}{\sqrt{105}} & -\frac{\sqrt{2}}{7\sqrt{3}} & -\frac{4}{7} \end{pmatrix}$	
$\langle\mathcal{A}_{10}\rangle$	$\mathrm{diag}(1,1,1)$	$\mathrm{diag}(1,1,1,1,1)$	$\mathrm{diag}(1,1,1,1,1)$	$\mathrm{diag}(1,1,1,1)$
$\langle\mathcal{A}_{11}\rangle$	$\mathrm{diag}\left(\tfrac{3}{2},1,\tfrac{1}{6}\right)$	$\mathrm{diag}\left(1,\tfrac{3}{2},1,\tfrac{1}{6},-1\right)$	$\mathrm{diag}\left(\tfrac{1}{6},\tfrac{3}{2},1,\tfrac{1}{6},-1\right)$	$\mathrm{diag}\left(-1,1,1,\tfrac{1}{6},-1\right)$
$\langle\mathcal{A}_{12}\rangle$	$\begin{pmatrix} 0 & \frac{9}{10} & \frac{\sqrt{21}}{5} \\ \frac{9}{10} & \frac{4}{5} & \frac{3\sqrt{21}}{70} \\ \frac{\sqrt{21}}{5} & \frac{3\sqrt{21}}{70} & \frac{116}{105} \end{pmatrix}$	$\begin{pmatrix} 0 & -\frac{9\sqrt{2}}{20} & -\frac{4}{5} & \frac{3\sqrt{6}}{20} & \frac{2\sqrt{2}}{5} \\ -\frac{9\sqrt{2}}{20} & \frac{9\sqrt{2}}{20} & \frac{9\sqrt{2}}{20} & -\frac{\sqrt{3}}{5} & 0 \\ -\frac{4}{5} & \frac{9\sqrt{2}}{20} & 0 & \frac{3\sqrt{6}}{28} & -\frac{4\sqrt{2}}{35} \\ \frac{3\sqrt{6}}{20} & -\frac{\sqrt{3}}{5} & \frac{3\sqrt{6}}{28} & \frac{58}{147} & \frac{18\sqrt{3}}{245} \\ \frac{2\sqrt{2}}{5} & 0 & -\frac{4\sqrt{2}}{35} & \frac{18\sqrt{3}}{245} & \frac{60}{49} \end{pmatrix}$	$\begin{pmatrix} 0 & \frac{\sqrt{7}}{5} & -\frac{3}{10} & -\frac{29\sqrt{2}}{15\sqrt{7}} & \frac{\sqrt{6}}{5\sqrt{7}} \\ \frac{\sqrt{7}}{5} & 0 & -\frac{9}{10\sqrt{7}} & -\frac{2\sqrt{2}}{5} & 0 \\ -\frac{3}{10} & -\frac{9}{10\sqrt{7}} & -\frac{4}{7} & \frac{3}{7\sqrt{14}} & -\frac{12\sqrt{6}}{35\sqrt{7}} \\ -\frac{29\sqrt{2}}{15\sqrt{7}} & -\frac{2\sqrt{2}}{5} & \frac{3}{7\sqrt{14}} & -\frac{58}{147} & \frac{17\sqrt{3}}{245} \\ \frac{\sqrt{6}}{5\sqrt{7}} & 0 & -\frac{12\sqrt{6}}{35\sqrt{7}} & \frac{17\sqrt{3}}{245} & \frac{10}{49} \end{pmatrix}$	$\begin{pmatrix} 0 & \frac{2}{5} & -\frac{3}{5\sqrt{14}} & -\frac{2\sqrt{21}}{7} \\ \frac{2}{5} & \frac{8}{35} & -\frac{\sqrt{27}}{35\sqrt{14}} & \frac{4\sqrt{21}}{49} \\ -\frac{3}{5\sqrt{14}} & -\frac{27}{35\sqrt{14}} & -\frac{493}{735} & \frac{\sqrt{3}}{49\sqrt{2}} \\ -\frac{2\sqrt{21}}{7} & \frac{4\sqrt{21}}{49} & \frac{\sqrt{3}}{49\sqrt{2}} & -\frac{32}{49} \end{pmatrix}$

TABLE XV. Matrix elements $\langle f|\mathcal{D}_k|i\rangle$ in various channels for operators $\mathcal{D}_k$ in the effective potentials.

Spin	$\langle\mathcal{D}_1\rangle$	$\langle\mathcal{D}_2\rangle$	$\langle\mathcal{D}_3\rangle$	$\langle\mathcal{D}_4\rangle$	$\langle\mathcal{D}_5\rangle$	$\langle\mathcal{D}_6\rangle$	$\langle\mathcal{D}_7\rangle$	$\langle\mathcal{D}_8\rangle$	$\langle\mathcal{D}_9\rangle$	$\langle\mathcal{D}_{10}\rangle$	$\langle\mathcal{D}_{11}\rangle$	$\langle\mathcal{D}_{12}\rangle$
$J=1/2$			(0)	$\left(-\sqrt{\frac{2}{3}}\right)$	(0)	$\left(-\sqrt{\frac{5}{3}}\right)$	(0)					
$J=3/2$	$\left(\sqrt{\frac{5}{2}}\right)$	(0)	(0)	$\left(-\sqrt{\frac{5}{3}}\right)$	(0)	$\left(-\sqrt{\frac{5}{6}}\right)$	(0)	$\left(\frac{1}{\sqrt{6}}\right)$	(0)	$\left(\frac{2}{5\sqrt{3}}\right)$	$\left(-\frac{\sqrt{3}}{2}\right)$	(0)
$J=5/2$								(1)	(0)	$\left(-\sqrt{\frac{8}{21}}\right)$	$\left(-\sqrt{\frac{7}{6}}\right)$	(0)

Spin	$\langle\mathcal{D}_{13}\rangle$	$\langle\mathcal{D}_{14}\rangle$	$\langle\mathcal{D}_{15}\rangle$	$\langle\mathcal{D}_{16}\rangle$	$\langle\mathcal{D}_{17}\rangle$	$\langle\mathcal{D}_{18}\rangle$	$\langle\mathcal{D}_{19}\rangle$	$\langle\mathcal{D}_{20}\rangle$	$\langle\mathcal{D}_{21}\rangle$	$\langle\mathcal{D}_{22}\rangle$	$\langle\mathcal{D}_{23}\rangle$	$\langle\mathcal{D}_{24}\rangle$
$J=1/2$	$\left(-\sqrt{\frac{5}{18}}\right)$	(0)	$\left(\sqrt{\frac{2}{3}}\right)$	(0)	$\left(-\sqrt{\frac{5}{3}}\right)$	(0)						
$J=3/2$	$\left(-\frac{2\sqrt{2}}{3}\right)$	(0)	$\left(\sqrt{\frac{5}{3}}\right)$	(0)	$\left(-\sqrt{\frac{5}{6}}\right)$	(0)	$\left(\sqrt{\frac{5}{2}}\right)$	(0)	$\left(\frac{1}{\sqrt{6}}\right)$	(0)	$\left(\frac{\sqrt{3}}{2}\right)$	(0)
$J=5/2$	$\left(-\sqrt{\frac{7}{6}}\right)$	(0)	(0)	$\left(\sqrt{\frac{2}{5}}\right)$	(0)	$\left(\sqrt{\frac{7}{15}}\right)$			(1)	(0)	$\left(\frac{\sqrt{3}}{2}\right)$	(0)

$$\mathcal{A}_6 = \mathcal{X}\mathcal{Y}(\boldsymbol{\epsilon}_{4m}^\dagger \cdot \boldsymbol{\epsilon}_{2a})\chi_3^\dagger S(\boldsymbol{\sigma}, i\boldsymbol{\epsilon}_{4n}^\dagger \times \boldsymbol{\epsilon}_{2b}, \hat{\boldsymbol{r}})\chi_1,$$

$$\mathcal{A}_7 = \mathcal{Z}\mathcal{T}\mathcal{Q}(\boldsymbol{\epsilon}_3^{\dagger m_2'} \cdot \boldsymbol{\epsilon}_1^{m_2})(\boldsymbol{\epsilon}_4^\dagger \cdot \boldsymbol{\epsilon}_2),$$

$$\mathcal{A}_8 = \mathcal{Z}\mathcal{T}\mathcal{Q}\left[(\boldsymbol{\epsilon}_3^{\dagger m_2'} \times \boldsymbol{\epsilon}_1^{m_2}) \cdot (\boldsymbol{\epsilon}_4^\dagger \times \boldsymbol{\epsilon}_2)\right],$$

$$\mathcal{A}_9 = \mathcal{Z}\mathcal{T}\mathcal{Q}S(\boldsymbol{\epsilon}_3^{\dagger m_2'} \times \boldsymbol{\epsilon}_1^{m_2}, \boldsymbol{\epsilon}_4^\dagger \times \boldsymbol{\epsilon}_2, \hat{\boldsymbol{r}}),$$

$$\mathcal{A}_{10} = \mathcal{X}\mathcal{Y}\mathcal{Z}\mathcal{T}\mathcal{Q}(\boldsymbol{\epsilon}_3^{\dagger m_2'} \cdot \boldsymbol{\epsilon}_1^{m_2})(\boldsymbol{\epsilon}_{4m}^\dagger \cdot \boldsymbol{\epsilon}_{2a})(\boldsymbol{\epsilon}_{4n}^\dagger \cdot \boldsymbol{\epsilon}_{2b}),$$

$$\mathcal{A}_{11} = \mathcal{X}\mathcal{Y}\mathcal{Z}\mathcal{T}\mathcal{Q}(\boldsymbol{\epsilon}_{4m}^\dagger \cdot \boldsymbol{\epsilon}_{2a})\left[(\boldsymbol{\epsilon}_3^{\dagger m_2'} \times \boldsymbol{\epsilon}_1^{m_2}) \cdot (\boldsymbol{\epsilon}_{4n}^\dagger \times \boldsymbol{\epsilon}_{2b})\right],$$

$$\mathcal{A}_{12} = \mathcal{X}\mathcal{Y}\mathcal{Z}\mathcal{T}\mathcal{Q}(\boldsymbol{\epsilon}_{4m}^\dagger \cdot \boldsymbol{\epsilon}_{2a})S(\boldsymbol{\epsilon}_3^{\dagger m_2'} \times \boldsymbol{\epsilon}_1^{m_2}, \boldsymbol{\epsilon}_{4n}^\dagger \times \boldsymbol{\epsilon}_{2b}, \hat{\boldsymbol{r}}).$$

Here, $\mathcal{X} = \sum_{m,n} C_{1m,1n}^{2,m+n}$, $\mathcal{Y} = \sum_{a,b} C_{1a,1b}^{2,a+b}$, $\mathcal{Z} = \sum_{m_1,m_2} C_{\frac{1}{2}m_1,1m_2}^{\frac{3}{2},m_1+m_2}$, $\mathcal{T} = \sum_{m_1',m_2'} C_{\frac{1}{2}m_1',1m_2'}^{\frac{3}{2},m_1'+m_2'}$, $Q = \chi_3^{\dagger m_1'}\chi_1^{m_1}$, and $S(\boldsymbol{x}, \boldsymbol{y}, \hat{\boldsymbol{r}}) = 3(\hat{\boldsymbol{r}} \cdot \boldsymbol{x})(\hat{\boldsymbol{r}} \cdot \boldsymbol{y}) - \boldsymbol{x} \cdot \boldsymbol{y}$. We present the corresponding matrix elements $\langle f|\mathcal{A}_k|i\rangle$ in Table XIV, which are obtained by sandwiching these operators between the relevant spin-orbit wave functions.

2. The effective potentials involved in $\Lambda_c\bar{D}_1(\bar{D}_2^*)$ systems

The OBE effective potentials in the analysis of the $\Lambda_c\bar{D}_1(\bar{D}_2^*)$ systems can be written as

$$\mathcal{V}^{\Lambda_c\bar{D}_1 \to \Lambda_c\bar{D}_1}(\mathbf{r}) = -2AY_\sigma\mathcal{A}_1 - \frac{1}{2}BY_\omega\mathcal{A}_1, \tag{B6}$$

$$\mathcal{V}^{\Lambda_c\bar{D}_2^* \to \Lambda_c\bar{D}_2^*}(\mathbf{r}) = -2AY_\sigma\mathcal{A}_4 - \frac{1}{2}BY_\omega\mathcal{A}_4, \tag{B7}$$

$$\mathcal{V}^{\Sigma_c\bar{D}_1 \to \Sigma_c\bar{D}_2^*}(\mathbf{r}) = -\frac{D\mathcal{H}(I)}{3\sqrt{6}}\left[\mathcal{D}_1\nabla^2 + \mathcal{D}_2 r\frac{\partial}{\partial r}\frac{1}{r}\frac{\partial}{\partial r}\right]Y_{P0} - \frac{2F\mathcal{G}(I)}{9\sqrt{6}}\left[2\mathcal{D}_1\nabla^2 - \mathcal{D}_2 r\frac{\partial}{\partial r}\frac{1}{r}\frac{\partial}{\partial r}\right]Y_{V0}, \tag{B8}$$

$$\mathcal{V}^{\Sigma_c\bar{D}_1 \to \Sigma_c^*\bar{D}_1}(\mathbf{r}) = -\frac{1}{\sqrt{3}}CY_{\sigma 1}\mathcal{D}_3 - \frac{1}{2\sqrt{3}}E\mathcal{G}(I)Y_{V1}\mathcal{D}_3 - \frac{5D\mathcal{H}(I)}{12\sqrt{3}}\left[\mathcal{D}_4\nabla^2 + \mathcal{D}_5 r\frac{\partial}{\partial r}\frac{1}{r}\frac{\partial}{\partial r}\right]Y_{P1}$$
$$+ \frac{5F\mathcal{G}(I)}{18\sqrt{3}}\left[2\mathcal{D}_4\nabla^2 - \mathcal{D}_5 r\frac{\partial}{\partial r}\frac{1}{r}\frac{\partial}{\partial r}\right]Y_{V1}, \tag{B9}$$

$$\mathcal{V}^{\Sigma_c\bar{D}_1 \to \Sigma_c^*\bar{D}_2^*}(\mathbf{r}) = -\frac{D\mathcal{H}(I)}{6\sqrt{2}}\left[\mathcal{D}_6\nabla^2 - \mathcal{D}_7 r\frac{\partial}{\partial r}\frac{1}{r}\frac{\partial}{\partial r}\right]Y_{P2} + \frac{F\mathcal{G}(I)}{9\sqrt{2}}\left[2\mathcal{D}_6\nabla^2 - \mathcal{D}_7 r\frac{\partial}{\partial r}\frac{1}{r}\frac{\partial}{\partial r}\right]Y_{V2}, \tag{B10}$$

$$\mathcal{V}^{\Sigma_c\bar{D}_2^* \to \Sigma_c^*\bar{D}_1}(\mathbf{r}) = -\frac{D\mathcal{H}(I)}{6\sqrt{2}}\left[\mathcal{D}_8\nabla^2 + \mathcal{D}_9 r\frac{\partial}{\partial r}\frac{1}{r}\frac{\partial}{\partial r}\right]Y_{P3} + \frac{F\mathcal{G}(I)}{9\sqrt{2}}\left[2\mathcal{D}_8\nabla^2 - \mathcal{D}_9 r\frac{\partial}{\partial r}\frac{1}{r}\frac{\partial}{\partial r}\right]Y_{V3}, \tag{B11}$$

$$\mathcal{V}^{\Sigma_c\bar{D}_2^* \to \Sigma_c^*\bar{D}_2^*}(\mathbf{r}) = -\frac{1}{\sqrt{3}}CY_{\sigma 4}\mathcal{D}_{10} - \frac{1}{2\sqrt{3}}E\mathcal{G}(I)Y_{V4}\mathcal{D}_{10} - \frac{D\mathcal{H}(I)}{2\sqrt{3}}\left[\mathcal{D}_{11}\nabla^2 + \mathcal{D}_{12} r\frac{\partial}{\partial r}\frac{1}{r}\frac{\partial}{\partial r}\right]Y_{P4}$$
$$+ \frac{E\mathcal{G}(I)}{3\sqrt{3}}\left[2\mathcal{D}_{11}\nabla^2 - \mathcal{D}_{12} r\frac{\partial}{\partial r}\frac{1}{r}\frac{\partial}{\partial r}\right]Y_{V4}, \tag{B12}$$

$$\mathcal{V}^{\Sigma_c^* \bar{D}_1 \to \Sigma_c^* \bar{D}_2^*}(\mathbf{r}) = \frac{D\mathcal{H}(I)}{2\sqrt{6}} \left[\mathcal{D}_{13}\nabla^2 + \mathcal{D}_{14} r \frac{\partial}{\partial r} \frac{1}{r} \frac{\partial}{\partial r} \right] Y_{P5} - \frac{F\mathcal{G}(I)}{3\sqrt{6}} \left[2\mathcal{D}_{13}\nabla^2 - \mathcal{D}_{14} r \frac{\partial}{\partial r} \frac{1}{r} \frac{\partial}{\partial r} \right] Y_{V5}, \tag{B13}$$

$$\mathcal{V}^{\Lambda_c \bar{D}_1 \to \Sigma_c \bar{D}_1}(\mathbf{r}) = -\frac{5G}{18\sqrt{2}} \left[\mathcal{A}_2\nabla^2 + \mathcal{A}_3 r \frac{\partial}{\partial r} \frac{1}{r} \frac{\partial}{\partial r} \right] Y_{\pi 6} - \frac{5H}{9\sqrt{2}} \left[2\mathcal{A}_2\nabla^2 - \mathcal{A}_3 r \frac{\partial}{\partial r} \frac{1}{r} \frac{\partial}{\partial r} \right] Y_{\rho 6}, \tag{B14}$$

$$\mathcal{V}^{\Lambda_c \bar{D}_1 \to \Sigma_c \bar{D}_2^*}(\mathbf{r}) = \frac{\sqrt{3}G}{18} \left[\mathcal{D}_1\nabla^2 + \mathcal{D}_2 r \frac{\partial}{\partial r} \frac{1}{r} \frac{\partial}{\partial r} \right] Y_{\pi 7} + \frac{\sqrt{3}H}{9} \left[2\mathcal{D}_1\nabla^2 - \mathcal{D}_2 r \frac{\partial}{\partial r} \frac{1}{r} \frac{\partial}{\partial r} \right] Y_{\rho 7}, \tag{B15}$$

$$\mathcal{V}^{\Lambda_c \bar{D}_1 \to \Sigma_c^* \bar{D}_1}(\mathbf{r}) = \frac{5\sqrt{6}}{12}G \left[\mathcal{D}_{15}\nabla^2 + \mathcal{D}_{16} r \frac{\partial}{\partial r} \frac{1}{r} \frac{\partial}{\partial r} \right] Y_{\pi 8} - \frac{5\sqrt{6}}{18}H \left[2\mathcal{D}_{15}\nabla^2 - \mathcal{D}_{16} r \frac{\partial}{\partial r} \frac{1}{r} \frac{\partial}{\partial r} \right] Y_{\rho 8}, \tag{B16}$$

$$\mathcal{V}^{\Lambda_c \bar{D}_1 \to \Sigma_c^* \bar{D}_2^*}(\mathbf{r}) = -\frac{G}{6} \left[\mathcal{D}_{17}\nabla^2 + \mathcal{D}_{18} r \frac{\partial}{\partial r} \frac{1}{r} \frac{\partial}{\partial r} \right] Y_{\pi 9} - \frac{H}{3} \left[2\mathcal{D}_{17}\nabla^2 - \mathcal{D}_{18} r \frac{\partial}{\partial r} \frac{1}{r} \frac{\partial}{\partial r} \right] Y_{\rho 9}, \tag{B17}$$

$$\mathcal{V}^{\Lambda_c \bar{D}_2^* \to \Sigma_c \bar{D}_1}(\mathbf{r}) = \frac{\sqrt{3}}{18}G \left[\mathcal{D}_{19}\nabla^2 + \mathcal{D}_{20} r \frac{\partial}{\partial r} \frac{1}{r} \frac{\partial}{\partial r} \right] Y_{\pi 10} + \frac{1}{3\sqrt{3}}H \left[2\mathcal{D}_{19}\nabla^2 - \mathcal{D}_{20} r \frac{\partial}{\partial r} \frac{1}{r} \frac{\partial}{\partial r} \right] Y_{\rho 10}, \tag{B18}$$

$$\mathcal{V}^{\Lambda_c \bar{D}_2^* \to \Sigma_c \bar{D}_2^*}(\mathbf{r}) = -\frac{\sqrt{2}G}{6} \left[\mathcal{A}_5\nabla^2 + \mathcal{A}_6 r \frac{\partial}{\partial r} \frac{1}{r} \frac{\partial}{\partial r} \right] Y_{\pi 11} + \frac{\sqrt{2}H}{3} \left[2\mathcal{A}_5\nabla^2 - \mathcal{A}_6 r \frac{\partial}{\partial r} \frac{1}{r} \frac{\partial}{\partial r} \right] Y_{\rho 11}, \tag{B19}$$

$$\mathcal{V}^{\Lambda_c \bar{D}_2^* \to \Sigma_c^* \bar{D}_1}(\mathbf{r}) = -\frac{G}{6} \left[\mathcal{D}_{21}\nabla^2 + \mathcal{D}_{22} r \frac{\partial}{\partial r} \frac{1}{r} \frac{\partial}{\partial r} \right] Y_{\pi 12} - \frac{H}{3} \left[2\mathcal{D}_{21}\nabla^2 - \mathcal{D}_{22} r \frac{\partial}{\partial r} \frac{1}{r} \frac{\partial}{\partial r} \right] Y_{\rho 12}, \tag{B20}$$

$$\mathcal{V}^{\Lambda_c \bar{D}_2^* \to \Sigma_c^* \bar{D}_2^*}(\mathbf{r}) = \frac{G}{\sqrt{6}} \left[\mathcal{D}_{23}\nabla^2 + \mathcal{D}_{24} r \frac{\partial}{\partial r} \frac{1}{r} \frac{\partial}{\partial r} \right] Y_{\pi 13} + \frac{\sqrt{6}H}{3} \left[2\mathcal{D}_{23}\nabla^2 - \mathcal{D}_{24} r \frac{\partial}{\partial r} \frac{1}{r} \frac{\partial}{\partial r} \right] Y_{\rho 13}. \tag{B21}$$

Here, the effective potentials in Eqs. (B8)–(B21) are only concerned with the coupled channel analysis. Of course, we need to emphasis that the relevant expressions of Appendix B 1 will also be involved in the coupled channel analysis. Variables q_i $(i = 0, 1, \ldots, 13)$ in the above OBE effective potentials are defined as

$$q_0 = \frac{m_{D_2^*}^2 - m_{D_1}^2}{2(m_{\Sigma_c} + m_{D_2^*})},$$

$$q_1 = \frac{m_{\Sigma_c^*}^2 - m_{\Sigma_c}^2}{2(m_{\Sigma_c^*} + m_{D_1})},$$

$$q_2 = \frac{m_{\Sigma_c^*}^2 + m_{D_1}^2 - m_{\Sigma_c}^2 - m_{D_2^*}^2}{2(m_{\Sigma_c^*} + m_{D_2^*})},$$

$$q_3 = \frac{m_{\Sigma_c^*}^2 + m_{D_2^*}^2 - m_{\Sigma_c}^2 - m_{D_1}^2}{2(m_{\Sigma_c^*} + m_{D_1})},$$

$$q_4 = \frac{m_{\Sigma_c^*}^2 - m_{\Sigma_c}^2}{2(m_{\Sigma_c^*} + m_{D_1})},$$

$$q_5 = \frac{m_{D_2^*}^2 - m_{D_1}^2}{2(m_{\Sigma_c^*} + m_{D_2^*})},$$

$$q_6 = \frac{m_{\Sigma_c}^2 - m_{\Lambda_c}^2}{2(m_{\Lambda_c} + m_{D_1})},$$

$$q_7 = \frac{m_{\Sigma_c}^2 + m_{D_1}^2 - m_{\Lambda_c}^2 - m_{D_2^*}^2}{2(m_{\Sigma_c} + m_{D_2^*})},$$

$$q_8 = \frac{m_{\Sigma_c^*}^2 - m_{\Lambda_c}^2}{2(m_{\Sigma_c^*} + m_{D_1})},$$

$$q_9 = \frac{m_{\Sigma_c^*}^2 + m_{D_1}^2 - m_{\Lambda_c}^2 - m_{D_2^*}^2}{2(m_{\Sigma_c^*} + m_{D_2^*})},$$

$$q_{10} = \frac{m_{\Sigma_c}^2 + m_{D_2^*}^2 - m_{\Lambda_c}^2 - m_{D_1}^2}{2(m_{\Sigma_c} + m_{D_1})},$$

$$q_{11} = \frac{m_{\Sigma_c}^2 - m_{\Lambda_c}^2}{2(m_{\Sigma_c} + m_{D_2^*})},$$

$$q_{12} = \frac{m_{\Sigma_c^*}^2 + m_{D_2^*}^2 - m_{\Lambda_c}^2 - m_{D_1}^2}{2(m_{\Sigma_c^*} + m_{D_1})},$$

$$q_{13} = \frac{m_{\Sigma_c^*}^2 - m_{\Lambda_c}^2}{2(m_{\Sigma_c^*} + m_{D_1})},$$

$$\Lambda_i^2 = \Lambda^2 - q_i^2, \quad m_{Ei}^2 = m_E^2 - q_i^2. \tag{B22}$$

In Eqs. (B8)–(B21), we also define several operators, i.e.,

$$\mathcal{D}_1 = \mathcal{X}(\boldsymbol{\epsilon}_{4m}^\dagger \cdot \boldsymbol{\epsilon}_2)\chi_3^\dagger(\boldsymbol{\sigma} \cdot \boldsymbol{\epsilon}_{4n}^\dagger)\chi_1,$$

$$\mathcal{D}_2 = \mathcal{X}(\boldsymbol{\epsilon}_{4m}^\dagger \cdot \boldsymbol{\epsilon}_2)\chi_3^\dagger S(\boldsymbol{\sigma}, \boldsymbol{\epsilon}_{4n}^\dagger, \hat{\boldsymbol{r}})\chi_1,$$

$$\mathcal{D}_3 = \mathcal{Z}\chi_3^{\dagger m_1}(\boldsymbol{\epsilon}_3^{\dagger m_2} \cdot \boldsymbol{\sigma})(\boldsymbol{\epsilon}_4^\dagger \cdot \boldsymbol{\epsilon}_2)\chi_1,$$

$$\mathcal{D}_4 = \mathcal{Z}\chi_3^{\dagger m_1}\left[(\boldsymbol{\epsilon}_3^{\dagger m_2} \times \boldsymbol{\sigma}) \cdot (\boldsymbol{\epsilon}_4^\dagger \times \boldsymbol{\epsilon}_2)\right]\chi_1,$$

$$\mathcal{D}_5 = \mathcal{Z}\chi_3^{\dagger m_1} S(\boldsymbol{\epsilon}_3^{\dagger m_2} \times \boldsymbol{\sigma}, \boldsymbol{\epsilon}_4^\dagger \times \boldsymbol{\epsilon}_2, \hat{\boldsymbol{r}})\chi_1,$$

$$\mathcal{D}_6 = \mathcal{X}\mathcal{Z}(\boldsymbol{\epsilon}_{4m}^\dagger \cdot \boldsymbol{\epsilon}_2)\chi_3^{\dagger m_1}\left[(i\boldsymbol{\epsilon}_3^{\dagger m_2} \times \boldsymbol{\sigma}) \cdot \boldsymbol{\epsilon}_{4n}^\dagger\right]\chi_1,$$

$$\mathcal{D}_7 = \mathcal{X}\mathcal{Z}(\boldsymbol{\epsilon}_{4m}^\dagger \cdot \boldsymbol{\epsilon}_2)\chi_3^{\dagger m_1} S(i\boldsymbol{\epsilon}_3^{\dagger m_2} \times \boldsymbol{\sigma}, \boldsymbol{\epsilon}_{4n}^\dagger, \hat{\boldsymbol{r}})\chi_1,$$

$$\mathcal{D}_8 = \mathcal{X}\mathcal{Z}(\boldsymbol{\epsilon}_4^\dagger \cdot \boldsymbol{\epsilon}_{2m})\chi_3^{\dagger m_1}\left[(i\boldsymbol{\epsilon}_3^\dagger \times \boldsymbol{\sigma}) \cdot \boldsymbol{\epsilon}_{2n}\right]\chi_1,$$

$$\mathcal{D}_9 = \mathcal{X}\mathcal{Z}(\boldsymbol{\epsilon}_4^\dagger \cdot \boldsymbol{\epsilon}_{2m})\chi_3^{\dagger m_1} S(i\boldsymbol{\epsilon}_3^\dagger \times \boldsymbol{\sigma}, \boldsymbol{\epsilon}_{2n}, \hat{\boldsymbol{r}})\chi_1,$$

$$\mathcal{D}_{10} = \mathcal{X}\mathcal{Y}\mathcal{Z}\chi_3^{\dagger m_1}\big(\boldsymbol{\epsilon}_3^{\dagger m_2}\cdot\boldsymbol{\sigma}\big)(\boldsymbol{\epsilon}_{4m}^{\dagger}\cdot\boldsymbol{\epsilon}_{2a})(\boldsymbol{\epsilon}_{4n}^{\dagger}\cdot\boldsymbol{\epsilon}_{2b})\chi_1,$$

$$\mathcal{D}_{11} = \mathcal{X}\mathcal{Y}\mathcal{Z}(\boldsymbol{\epsilon}_{4m}^{\dagger}\cdot\boldsymbol{\epsilon}_{2a})\chi_3^{\dagger m_1}\big[\big(\boldsymbol{\epsilon}_3^{\dagger m_2}\times\boldsymbol{\sigma}\big)\cdot(\boldsymbol{\epsilon}_{4n}^{\dagger}\times\boldsymbol{\epsilon}_{2b})\big]\chi_1,$$

$$\mathcal{D}_{12} = \mathcal{X}\mathcal{Y}\mathcal{Z}(\boldsymbol{\epsilon}_{4m}^{\dagger}\cdot\boldsymbol{\epsilon}_{2a})\chi_3^{\dagger m_1}S\big(\boldsymbol{\epsilon}_3^{\dagger m_2}\times\boldsymbol{\sigma},\boldsymbol{\epsilon}_{4n}^{\dagger}\times\boldsymbol{\epsilon}_{2b},\hat{\boldsymbol{r}}\big)\chi_1,$$

$$\mathcal{D}_{13} = \mathcal{X}\mathcal{Z}\mathcal{T}\mathcal{Q}(\boldsymbol{\epsilon}_{4m}^{\dagger}\cdot\boldsymbol{\epsilon}_2)\big[i\big(\boldsymbol{\epsilon}_3^{\dagger m_2'}\times\boldsymbol{\epsilon}_1^{m_2}\big)\cdot\boldsymbol{\epsilon}_{4n}^{\dagger}\big],$$

$$\mathcal{D}_{14} = \mathcal{X}\mathcal{Z}\mathcal{T}\mathcal{Q}(\boldsymbol{\epsilon}_{4m}^{\dagger}\cdot\boldsymbol{\epsilon}_2)S\big(i\boldsymbol{\epsilon}_3^{\dagger m_2'}\times\boldsymbol{\epsilon}_1^{m_2},\boldsymbol{\epsilon}_{4n}^{\dagger},\hat{\boldsymbol{r}}\big),$$

$$\mathcal{D}_{15} = \mathcal{Z}\chi_3^{\dagger m_1}\big[i\boldsymbol{\epsilon}_3^{\dagger m_2}\cdot(\boldsymbol{\epsilon}_4^{\dagger}\times\boldsymbol{\epsilon}_2)\big]\chi_1,$$

$$\mathcal{D}_{16} = \mathcal{Z}\chi_3^{\dagger m_1}S\big(i\boldsymbol{\epsilon}_3^{\dagger m_2},\boldsymbol{\epsilon}_4^{\dagger}\times\boldsymbol{\epsilon}_2,\hat{\boldsymbol{r}}\big)\chi_1,$$

$$\mathcal{D}_{17} = \mathcal{X}\mathcal{Z}(\boldsymbol{\epsilon}_{4m}^{\dagger}\cdot\boldsymbol{\epsilon}_2)\chi_3^{\dagger m_1}\big(\boldsymbol{\epsilon}_3^{\dagger m_2}\cdot\boldsymbol{\epsilon}_{4n}^{\dagger}\big)\chi_1,$$

$$\mathcal{D}_{18} = \mathcal{X}\mathcal{Z}(\boldsymbol{\epsilon}_{4m}^{\dagger}\cdot\boldsymbol{\epsilon}_2)\chi_3^{\dagger m_1}S\big(\boldsymbol{\epsilon}_3^{\dagger m_2},\boldsymbol{\epsilon}_{4n}^{\dagger},\hat{\boldsymbol{r}}\big)\chi_1,$$

$$\mathcal{D}_{19} = \mathcal{X}(\boldsymbol{\epsilon}_4^{\dagger}\cdot\boldsymbol{\epsilon}_{2m})\chi_3^{\dagger}(\boldsymbol{\sigma}\cdot\boldsymbol{\epsilon}_{2n})\chi_1,$$

$$\mathcal{D}_{20} = \mathcal{X}(\boldsymbol{\epsilon}_4^{\dagger}\cdot\boldsymbol{\epsilon}_{2m})\chi_3^{\dagger}S(\boldsymbol{\sigma},\boldsymbol{\epsilon}_{2n},\hat{\boldsymbol{r}})\chi_1,$$

$$\mathcal{D}_{21} = \mathcal{X}\mathcal{Z}(\boldsymbol{\epsilon}_4^{\dagger}\cdot\boldsymbol{\epsilon}_{2m})\chi_3^{\dagger m_1}\big(\boldsymbol{\epsilon}_3^{\dagger m_2}\cdot\boldsymbol{\epsilon}_{2n}\big)\chi_1,$$

$$\mathcal{D}_{22} = \mathcal{X}\mathcal{Z}(\boldsymbol{\epsilon}_4^{\dagger}\cdot\boldsymbol{\epsilon}_{2m})\chi_3^{\dagger m_1}S\big(\boldsymbol{\epsilon}_3^{\dagger m_2},\boldsymbol{\epsilon}_{2n},\hat{\boldsymbol{r}}\big)\chi_1,$$

$$\mathcal{D}_{23} = \mathcal{X}\mathcal{Y}\mathcal{Z}(\boldsymbol{\epsilon}_{4m}^{\dagger}\cdot\boldsymbol{\epsilon}_{2a})\chi_3^{\dagger m_1}\big[i\boldsymbol{\epsilon}_3^{\dagger m_2}\cdot(\boldsymbol{\epsilon}_{4n}^{\dagger}\times\boldsymbol{\epsilon}_{2b})\big]\chi_1,$$

$$\mathcal{D}_{24} = \mathcal{X}\mathcal{Y}\mathcal{Z}(\boldsymbol{\epsilon}_{4m}^{\dagger}\cdot\boldsymbol{\epsilon}_{2a})\chi_3^{\dagger m_1}S\big(\boldsymbol{\epsilon}_3^{\dagger m_2},i\boldsymbol{\epsilon}_{4n}^{\dagger}\times\boldsymbol{\epsilon}_{2b},\hat{\boldsymbol{r}}\big)\chi_1.$$

The operators $\mathcal{D}_k$ ($k = 1, 2, \ldots, 24$) are only concerned with the coupled channel analysis. In Table XV, we collect the relevant numerical matrices $\langle f|\mathcal{D}_k|i\rangle$ for these operators $\mathcal{D}_k$.

[1] H. X. Chen, W. Chen, X. Liu, and S. L. Zhu, The hidden-charm pentaquark and tetraquark states, Phys. Rep. **639**, 1 (2016).

[2] X. Liu, An overview of XYZ new particles, Chin. Sci. Bull. **59**, 3815 (2014).

[3] Y. R. Liu, H. X. Chen, W. Chen, X. Liu, and S. L. Zhu, Pentaquark and tetraquark states, Prog. Part. Nucl. Phys. **107**, 237 (2019).

[4] S. L. Olsen, T. Skwarnicki, and D. Zieminska, Nonstandard heavy mesons and baryons: Experimental evidence, Rev. Mod. Phys. **90**, 015003 (2018).

[5] F. K. Guo, C. Hanhart, Ulf-G. Meißner, Q. Wang, Q. Zhao, and B. S. Zou, Hadronic molecules, Rev. Mod. Phys. **90**, 015004 (2018).

[6] C. Hanhart, Theory of hadronic molecules applied to the XYZ states, EPJ Web Conf. **218**, 08002 (2019).

[7] R. Aaij *et al.* (LHCb Collaboration), Observation of a Narrow Pentaquark State, $P_c(4312)^+$, and of Two-Peak Structure of the $P_c(4450)^+$, Phys. Rev. Lett. **122**, 222001 (2019).

[8] R. Aaij *et al.* (LHCb Collaboration), Observation of J/ψ Resonances Consistent with Pentaquark States in $\Lambda_b^0 \to J/\psi K^- p$ Decays, Phys. Rev. Lett. **115**, 072001 (2015).

[9] R. Chen, X. Liu, X. Q. Li, and S. L. Zhu, Identifying Exotic Hidden-Charm Pentaquarks, Phys. Rev. Lett. **115**, 132002 (2015).

[10] H. X. Chen, W. Chen, X. Liu, T. G. Steele, and S. L. Zhu, Towards Exotic Hidden-charm Pentaquarks in QCD, Phys. Rev. Lett. **115**, 172001 (2015).

[11] M. Karliner and J. L. Rosner, New Exotic Meson and Baryon Resonances from Doubly-Heavy Hadronic Molecules, Phys. Rev. Lett. **115**, 122001 (2015).

[12] L. Roca, J. Nieves, and E. Oset, LHCb pentaquark as a $\bar{D}^*\Sigma_c$-$\bar{D}^*\Sigma_c^*$ molecular state, Phys. Rev. D **92**, 094003 (2015).

[13] A. Mironov and A. Morozov, Is the pentaquark doublet a hadronic molecule? JETP Lett. **102**, 271 (2015).

[14] J. He, $\bar{D}\Sigma_c^*$ and $\bar{D}^*\Sigma_c$ interactions and the LHCb hidden-charmed pentaquarks, Phys. Lett. B **753**, 547 (2016).

[15] U. G. Meißner and J. A. Oller, Testing the $\chi_{c1}p$ composite nature of the $P_c(4450)$, Phys. Lett. B **751**, 59 (2015).

[16] T. J. Burns, Phenomenology of $P_c(4380)^+$, $P_c(4450)^+$ and related states, Eur. Phys. J. A **51**, 152 (2015).

[17] Y. Shimizu, D. Suenaga, and M. Harada, Coupled channel analysis of molecule picture of $P_c(4380)$, Phys. Rev. D **93**, 114003 (2016).

[18] R. Chen, X. Liu, and S. L. Zhu, Hidden-charm molecular pentaquarks and their charm-strange partners, Nucl. Phys. A **954**, 406 (2016).

[19] M. I. Eides, V. Y. Petrov, and M. V. Polyakov, Narrow nucleon-$\phi(2S)$ bound state and LHCb pentaquarks, Phys. Rev. D **93**, 054039 (2016).

[20] H. Huang, C. Deng, J. Ping, and F. Wang, Possible pentaquarks with heavy quarks, Eur. Phys. J. C **76**, 624 (2016).

[21] H. X. Chen, E. L. Cui, W. Chen, X. Liu, T. G. Steele, and S. L. Zhu, QCD sum rule study of hidden-charm pentaquarks, Eur. Phys. J. C **76**, 572 (2016).

[22] G. Yang and J. Ping, The structure of pentaquarks P_c^+ in the chiral quark model, Phys. Rev. D **95**, 014010 (2017).

[23] J. He, Understanding spin parity of $P_c(4450)$ and $Y(4274)$ in a hadronic molecular state picture, Phys. Rev. D **95**, 074004 (2017).

[24] Y. Yamaguchi and E. Santopinto, Hidden-charm pentaquarks as a meson-baryon molecule with coupled channels for $\bar{D}^{(*)}\Lambda_c$ and $\bar{D}^{(*)}\Sigma_c^{(*)}$, Phys. Rev. D **96**, 014018 (2017).

[25] J. M. Richard, A. Valcarce, and J. Vijande, Stable heavy pentaquarks in constituent models, Phys. Lett. B **774**, 710 (2017).

[26] Z. C. Yang, Z. F. Sun, J. He, X. Liu, and S. L. Zhu, The possible hidden-charm molecular baryons composed of anti-charmed meson and charmed baryon, Chin. Phys. C **36**, 6 (2012).

[27] J. J. Wu, R. Molina, E. Oset, and B. S. Zou, Prediction of Narrow N^* and Λ^* Resonances with Hidden Charm Above 4 GeV, Phys. Rev. Lett. **105**, 232001 (2010).

[28] W. L. Wang, F. Huang, Z. Y. Zhang, and B. S. Zou, $\Sigma_c\bar{D}$ and $\Lambda_c\bar{D}$ states in a chiral quark model, Phys. Rev. C **84**, 015203 (2011).

[29] J. J. Wu, T.-S. H. Lee, and B. S. Zou, Nucleon resonances with hidden charm in coupled-channel models, Phys. Rev. C **85**, 044002 (2012).

[30] R. Chen, Z. F. Sun, X. Liu, and S. L. Zhu, Strong LHCb evidence supporting the existence of the hidden-charm molecular pentaquarks, Phys. Rev. D **100**, 011502 (2019).

[31] H. X. Chen, W. Chen, and S. L. Zhu, Possible interpretations of the $P_c(4312)$, $P_c(4440)$, and $P_c(4457)$, Phys. Rev. D **100**, 051501 (2019).

[32] M. Z. Liu, Y. W. Pan, F. Z. Peng, M. S. Sønchez, L. S. Geng, A. Hosaka, and M. Pavon Valderrama, Emergence of a Complete Heavy-Quark Spin Symmetry Multiplet: Seven Molecular Pentaquarks in Light of the Latest LHCb Analysis, Phys. Rev. Lett. **122**, 242001 (2019).

[33] J. He, Study of $P_c(4457)$, $P_c(4440)$, and $P_c(4312)$ in a quasipotential Bethe-Salpeter equation approach, Eur. Phys. J. C **79**, 393 (2019).

[34] C. W. Xiao, J. Nieves, and E. Oset, Heavy quark spin symmetric molecular states from $\bar{D}^{(*)}\Sigma_c^{(*)}$ and other coupled channels in the light of the recent LHCb pentaquarks, Phys. Rev. D **100**, 014021 (2019).

[35] Z. H. Guo and J. A. Oller, Anatomy of the newly observed hidden-charm pentaquark states: $P_c(4312)$, $P_c(4440)$ and $P_c(4457)$, Phys. Lett. B **793**, 144 (2019).

[36] H. Huang, J. He, and J. Ping, Looking for the hidden-charm pentaquark resonances in $J/\psi p$ scattering, arXiv:1904.00221.

[37] Y. Shimizu, Y. Yamaguchi, and M. Harada, Heavy quark spin multiplet structure of $P_c(4312)$, $P_c(4440)$, and $P_c(4457)$, arXiv:1904.00587.

[38] C. J. Xiao, Y. Huang, Y. B. Dong, L. S. Geng, and D. Y. Chen, Exploring the molecular scenario of $P_c(4312)$, $P_c(4440)$, and $P_c(4457)$, Phys. Rev. D **100**, 014022 (2019).

[39] L. Meng, B. Wang, G. J. Wang, and S. L. Zhu, The hidden charm pentaquark states and $\Sigma_c\bar{D}^{(*)}$ interaction in chiral perturbation theory, Phys. Rev. D **100**, 014031 (2019).

[40] T. J. Burns and E. S. Swanson, Molecular interpretation of the $P_c(4440)$ and $P_c(4457)$ states, Phys. Rev. D **100**, 114033 (2019).

[41] Y. W. Pan, M. Z. Liu, F. Z. Peng, M. S. Sønchez, L. S. Geng, and M. Pavon Valderrama, Model independent determination of the spins of the $P_c(4440)$ and $P_c(4457)$ from the spectroscopy of the triply charmed dibaryons, arXiv:1907.11220.

[42] M. Z. Liu, T. W. Wu, M. S. Sønchez, M. P. Valderrama, L. S. Geng, and J. J. Xie, Spin-parities of the $P_c(4440)$ and $P_c(4457)$ in the one-boson-exchange model, arXiv:1907.06093.

[43] Y. J. Xu, C. Y. Cui, Y. L. Liu, and M. Q. Huang, The partial decay width of $P_c(4312)$ as a $\bar{D}\Sigma_c$ molecular state, arXiv:1907.05097.

[44] M. Pavon Valderrama, One pion exchange and the quantum numbers of the $P_c(4440)$ and $P_c(4457)$ pentaquarks, Phys. Rev. D **100**, 094028 (2019).

[45] Z. G. Wang and X. Wang, Analysis of the strong decays of the $P_c(4312)$ as a pentaquark molecular state with QCD sum rules, arXiv:1907.04582.

[46] Y. Yamaguchi, H. Garcła-Tecocoatzi, A. Giachino, A. Hosaka, E. Santopinto, S. Takeuchi, and M. Takizawa, Heavy quark spin symmetry with chiral tensor dynamics in the light of the recent LHCb pentaquarks, arXiv:1907.04684.

[47] J. B. Cheng and Y. R. Liu, $P_c(4457)^+$, $P_c(4440)^+$, and $P_c(4312)^+$: Molecules or compact pentaquarks? Phys. Rev. D **100**, 054002 (2019).

[48] M. L. Du, V. Baru, F. K. Guo, C. Hanhart, U. G. Meißner, J. A. Oller, and Q. Wang, Evidence that the LHCb P_c states are hadronic molecules and the existence of a narrow $P_c(4380)$, arXiv:1910.11846.

[49] X. Liu, Y. R. Liu, W. Z. Deng, and S. L. Zhu, Is $Z^+(4430)$ a loosely bound molecular state? Phys. Rev. D **77**, 034003 (2008).

[50] X. Liu, Y. R. Liu, W. Z. Deng, and S. L. Zhu, $Z^+(4430)$ as a $D_1'D^*(D_1D^*)$ molecular state, Phys. Rev. D **77**, 094015 (2008).

[51] L. L. Shen, X. L. Chen, Z. G. Luo, P. Z. Huang, S. L. Zhu, P. F. Yu, and X. Liu, The molecular systems composed of the charmed mesons in the $H\bar{S} + h.c.$ doublet, Eur. Phys. J. C **70**, 183 (2010).

[52] B. Hu, X. L. Chen, Z. G. Luo, P. Z. Huang, S. L. Zhu, P. F. Yu, and X. Liu, Possible heavy molecular states composed of a pair of excited charm-strange mesons, Chin. Phys. C **35**, 113 (2011).

[53] R. Chen, X. Liu, Y. R. Liu, and S. L. Zhu, Predictions of the hidden-charm molecular states with four-quark component, Eur. Phys. J. C **76**, 319 (2016).

[54] X. Liu, Z. G. Luo, and S. L. Zhu, Novel charmonium-like structures in the $J/\psi\phi$ and $J/\psi\omega$ invariant mass spectra, Phys. Lett. B **699**, 341 (2011); **707**, 577(E) (2012).

[55] S. K. Choi *et al.* (Belle Collaboration), Observation of a Narrow Charmoniumlike State in Exclusive $B^\pm \rightarrow K^\pm\pi^+\pi^-J/\psi$ Decays, Phys. Rev. Lett. **91**, 262001 (2003).

[56] K. Abe *et al.* (Belle Collaboration), Observation of a Near-Threshold $\omega J/\psi$ Mass Enhancement in Exclusive $B \rightarrow K\omega J/\psi$ Decays, Phys. Rev. Lett. **94**, 182002 (2005).

[57] S. K. Choi *et al.* (Belle Collaboration), Observation of a Resonancelike Structure in the $pi^\pm\psi'$ Mass Distribution in Exclusive $B \rightarrow K\pi^\pm\psi'$ Decays, Phys. Rev. Lett. **100**, 142001 (2008).

[58] R. Mizuk *et al.* (Belle Collaboration), Observation of two resonancelike structures in the $\pi^+\chi_{c1}$ mass distribution in exclusive $\bar{B}_0 \rightarrow K^-\pi^+\chi_{c1}$ decays, Phys. Rev. D **78**, 072004 (2008).

[59] T. Aaltonen *et al.* (CDF Collaboration), Evidence for a Narrow Near-Threshold Structure in the $J/\psi\phi$ Mass Spectrum in $B^+ \rightarrow J/\psi\phi K^+$ Decays, Phys. Rev. Lett. **102**, 242002 (2009).

[60] R. Aaij *et al.* (LHCb Collaboration), Observation of the Resonant Character of the $Z(4430)^-$ State, Phys. Rev. Lett. **112**, 222002 (2014).

[61] K. Chilikin *et al.* (Belle Collaboration), Observation of a new charged charmoniumlike state in $\bar{B}^0 \rightarrow J/\phi K^-\pi^+$ decays, Phys. Rev. D **90**, 112009 (2014).

[62] R. Aaij *et al.* (LHCb Collaboration), Observation of $J/\psi\phi$ Structures Consistent with Exotic States from Amplitude Analysis of $B^+ \rightarrow J/\psi\phi K^+$ Decays, Phys. Rev. Lett. **118**, 022003 (2017).

[63] R. Aaij *et al.* (LHCb Collaboration), Amplitude analysis of $B^+ \rightarrow J/\psi\phi K^+$ decays, Phys. Rev. D **95**, 012002 (2017).

[64] R. Aaij *et al.* (LHCb Collaboration), Evidence for an $\eta_c(1S)\pi^-$ resonance in $B^0 \rightarrow \eta_c(1S)K^+\pi^-$ decays, Eur. Phys. J. C **78**, 1019 (2018).

[65] M. Tanabashi *et al.* (Particle Data Group), Review of particle physics, Phys. Rev. D **98**, 030001 (2018).

[66] N. A. Tornqvist, From the deuteron to deusons, an analysis of deuteronlike meson-meson bound states, Z. Phys. C **61**, 525 (1994).

[67] N. A. Tornqvist, On deusons or deuteronlike meson-meson bound states, Nuovo Cim. A **107**, 2471 (1994).

[68] Y. R. Liu and M. Oka, $\Lambda_c N$ bound states revisited, Phys. Rev. D **85**, 014015 (2012).

[69] G. J. Ding, Are $Y(4260)$ and $Z_2^+(4250)$ D_1D or D_0D^* hadronic molecules? Phys. Rev. D **79**, 014001 (2009).

[70] M. B. Wise, Chiral perturbation theory for hadrons containing a heavy quark, Phys. Rev. D **45**, R2188 (1992).

[71] R. Casalbuoni, A. Deandrea, N. Di Bartolomeo, R. Gatto, F. Feruglio, and G. Nardulli, Light vector resonances in the effective chiral Lagrangian for heavy mesons, Phys. Lett. B **292**, 371 (1992).

[72] R. Casalbuoni, A. Deandrea, N. Di Bartolomeo, R. Gatto, F. Feruglio, and G. Nardulli, Phenomenology of heavy meson chiral Lagrangians, Phys. Rep. **281**, 145 (1997).

[73] T. M. Yan, H. Y. Cheng, C. Y. Cheung, G. L. Lin, Y. C. Lin, and H. L. Yu, Heavy quark symmetry and chiral dynamics, Phys. Rev. D **46**, 1148 (1992); **55**, 5851(E) (1997).

[74] A. F. Falk and M. E. Luke, Strong decays of excited heavy mesons in chiral perturbation theory, Phys. Lett. B **292**, 119 (1992).

[75] D. O. Riska and G. E. Brown, Nucleon resonance transition couplings to vector mesons, Nucl. Phys. A **679**, 577 (2001).

[76] F. L. Wang, R. Chen, Z. W. Liu, and X. Liu, Possible triple-charm molecular pentaquarks from $\Xi_{cc}D_1/\Xi_{cc}D_2^*$ interactions, Phys. Rev. D **99**, 054021 (2019).

[77] R. Chen, A. Hosaka, and X. Liu, Prediction of triple-charm molecular pentaquarks, Phys. Rev. D **96**, 114030 (2017).

[78] E. Epelbaum, W. Gloeckle, and U. G. Meißner, Nuclear forces from chiral Lagrangians using the method of unitary transformation. 2. The two nucleon system, Nucl. Phys. A **671**, 295 (2000).

[79] J. Bsaisou, J. de Vries, C. Hanhart, S. Liebig, U. G. Meißner, D. Minossi, A. Nogga, and A. Wirzba, Nuclear electric dipole moments in chiral effective field theory, J. High Energy Phys. 03 (2015) 104.

[80] H. Y. Cheng and K. C. Yang, Charmless hadronic B decays into a tensor meson, Phys. Rev. D **83**, 034001 (2011).

[81] R. Chen, J. He, and X. Liu, Possible strange hidden-charm pentaquarks from $\Sigma_c^{(*)}\bar{D}_s^*$ and $\Xi_c^{(',*)}\bar{D}^*$ interactions, Chin. Phys. C **41**, 103105 (2017).

[82] R. Chen, A. Hosaka, and X. Liu, Heavy molecules and one-σ/ω-exchange model, Phys. Rev. D **96**, 116012 (2017).

[83] N. Li and S. L. Zhu, Hadronic molecular states composed of heavy flavor baryons, Phys. Rev. D **86**, 014020 (2012).

[84] R. Chen, A. Hosaka, and X. Liu, Searching for possible Ω_c-like molecular states from meson-baryon interaction, Phys. Rev. D **97**, 036016 (2018).

[85] E. Klempt, F. Bradamante, A. Martin, and J. M. Richard, Antinucleon nucleon interaction at low energy: Scattering and protonium, Phys. Rep. **368**, 119 (2002).

[86] R. Aaij *et al.* (LHCb Collaboration), Observation of the decay $\Lambda_b^0 \to \psi(2S)p\pi^-$, J. High Energy Phys. 08 (2018) 131.